A First Course on Aerodynamics

Arnab Roy

Arnab Roy

A First Course on Aerodynamics

A First Course on Aerodynamics

ISBN 978-87-7681-926-2

Contents

1 Fundamental Concepts in Aerodynamics and Inviscid Incompressible Flow

1.1 Introduction

A brief introduction is provided in this section about Aerodynamics in general. However, the focus is mainly on low speed flow. Concepts have been introduced without too much rigor. This would hopefully help the reader to get a first glimpse of the subject without getting into too many details. Figures have been used to explain concepts wherever possible. Lengthy derivations have been avoided because reference books could be used for that purpose. Main equations to remember have been provided straight away with relevant explanation.

The main concentration in this chapter is on introducing some basic concepts, discussion on low speed flow past airfoils and finite wings, forces and moments that are developed on these bodies due to air flow and a brief exposure to some of the methods of analyzing these flows.

1.2 Definition and approach

The subject 'Aerodynamics' relates to the study of relative flow of air past an aircraft or any other object of interest like train, automobile, building etc. The term 'air' is used in a generic sense. It basically means the flowing gaseous medium which could be air, helium or any other gas for that matter depending on situation. An aircraft is a body which is able to fly because of aerodynamic forces and moments generated by the action of air flowing past it. This flow of air could be due to the motion of an aircraft through air during flight or due to the motion of flowing air past an aircraft model fixed in the test section of a wind tunnel. Aerodynamics is an important branch of Aerospace Engineering.

There are three components in modern aerodynamic studies. They are experimental, theoretical (analytical or semi analytical) and computational fluid dynamics (CFD) approaches respectively. Each approach has its own advantages and disadvantages. Usually the most effective approach is to amalgamate both experimental and theoretical/ CFD investigation in a most rational manner to solve a particular problem.

Experimental studies are conducted in wind tunnels. Wind tunnels are used to perform aerodynamic measurements on scaled down models of prototypes. Usually measurement of pressure on model surface, forces and moments acting on the model, wake survey, flow visualisation etc are performed to obtain valuable understanding of the flow problem. The main disadvantages of experimental approach are high capital and running cost of wind tunnels, skill required in manufacturing models accurately and in acquisition of data, interpretation of data etc. Another major drawback is due to the difficulty of simultaneously maintaining the Mach number and Reynolds number experienced in flight. Mach number is the ratio of relative air velocity and speed of sound through air. Reynolds number is the ratio of inertia force and viscous force. It is a well known fact that in order to maintain dynamic similarity between the flow past a scaled down model in a wind tunnel and that around an actual prototype in flight one needs to maintain equality of the above non dimensional numbers. If they are not simultaneously satisfied, there would be some differences in the flow character between the two situations and therefore corrections would have to be made in the wind tunnel data before they could be used.

Theoretical and CFD studies have led to valuable understanding of wide range of flow problems till date. However, these approaches suffer from some limitations too. The basic limitation stems from the fact that the governing equation of real viscous compressible flow around a body, the Navier-Stokes equations can not in general be solved theoretically. Navier-Stokes equations, in principle, are capable of giving a totally adequate description of all flow regimes of interest to the aerodynamicist. However, that needs highly accurate numerical solution of governing equations subject to suitable initial and boundary conditons. Stringent accuracy requirements make the computations extremely expensive and therefore impractical to pursue on a routine basis. Therefore, very often, instead of solving the full Navier Stokes equations its simplified forms are used. Following this approach, the simplest form under assumption of inviscid (infinite Reynolds number, where the effect of viscosity is zero), incompressible (zero Mach number) and irrotational flow (we will discuss it little later in this chapter) is the Laplace equation which is significantly easier to solve numerically as compared to Navier Stokes equations and can give valuable inputs about certain flow problems. A variety of correction schemes have also been developed to incorporate effects due to viscosity and compressibility in the solution of Laplace equation. These 'correction schemes' have played an important role in providing alternative solutions to Navier-Stokes equation. In this chapter we would look at Laplace equation as a tool for solving potential flow problems and how it could help us in predicting inviscid incompressible irrotational flow past airfoils.

1.3 Fundamental concepts

1.3.1 Forces and Moments acting on an airfoil

In aerodynamic studies the air speed is usually designated as free stream speed U_∞. The subscript ∞ suggests that flow at infinite distance from the aircraft is completely unaffected by the presence of the aircraft. As the flow approaches the aircraft, it gets disturbed and the local velocity on the surface of the aircraft is changed or perturbed. At different points on the surface of the aircraft, different values of velocity will be observed which may be significantly different from U_∞. Consequently the pressure distribution on the surface of the aircraft will vary from the undisturbed pressure of the free stream at infinity.

The only two mechanisms nature has for communicating to a body moving through a fluid are pressure and shear stress distribution on its surface. The main focus of aerodynamics is determination of pressure and shear stress distribution around such a body surface and integrating their distribution to obtain the resultant force and moment acting on the body. Pressure acts normal to the surface of the body while shear stress acts tangential to it. Pressure on the upper surface of the wing of an aircraft is usually lower and on the lower surface it is higher. This difference in pressure between the two surfaces provides the necessary lift force which keeps the aircraft afloat during flight. In the simplest form of motion of an aircraft, i.e., straight and level unaccelerated flight, equilibrium is maintained between the weight and lift force and engine thrust and drag force. Shear stress acts tangential to the body surface and it arises due to the viscous nature of the flow. It acts in the direction of the flow and has an effect of slowing down the relative flow between the body and the fluid. Due to this stress the relative flow comes to a perfect halt at the body surface, at least at comparatively lower free stream speeds. The effect of viscous stresses is felt within a small region near the body boundary (called as boundary layer) where the velocity changes rapidly from zero at the wall to free stream velocity some distance away from the wall in the surface normal direction. Viscous stresses are proportional to coefficient of viscosity and velocity gradients. Beyond this region the flow behaves as through it is inviscid (devoid of viscosity) in nature. Even though the fluid characteristics remain unchanged in that region, i.e., the fluid viscosity is not reduced (actually there is no reason for it to reduce!), the flow seems to behave like an inviscid one because the velocity gradients have vanished. Therefore it makes sense to develop theories to handle inviscid flow.

In general the resultant force and moment acting on an aircraft in motion could be resolved into three components each. Resultant force could be resolved into lift, drag and side force and resultant moment could be resolved into pitching moment, rolling moment and yawing moment respectively. Lift force (L) acts upwards perpendicular to the direction of flight or undisturbed stream. Drag force (D) acts in the opposite direction to the line of flight or in the same direction as the motion of the undisturbed stream. It is the force which resists the motion of the aircraft. Side force acts in the spanwise direction of the aircraft and is considered to be positive when it acts towards the star-board wing tip. Pitching moment (M) acts in the plane containing the lift and the drag i.e. in the vertical plane when the aircraft is flying horizontally. It is positive when it tends to raise the aircraft nose upwards. Rolling Moment is the moment tending to make the aircraft roll about the flight direction i.e. tending to depress one wing tip and raise the other. It is positive when it tends to depress the starboard wing tip. Yawing moment tends to rotate the aircraft about the lift direction, i.e., to swing the nose to one side or to other of the flight direction. It is positive when it swings or tends to swing the nose to the right.

The main components of an aircraft are wing, fuselage, horizontal tail-plane and vertical tail-plane. The aerodynamic behavior of an aircraft depends very strongly on its wing. The section of the wing is called as airfoil or aerofoil. The airfoil nomenclature is shown in Figure 1.1. As is evident from the figure a certain thickness is disposed equally around the so called 'mean camber line' to produce the airfoil shape. One can also notice that there is a particular location for maximum thickness and camber. When the mean camber line is coincident with the mean chord line we get a symmetric airfoil, otherwise we get a cambered airfoil. The airfoil shown in Figure 1.1 is a cambered airfoil. Figure 1.2 shows the pressure and shear stress acting on a small elemental length 'ds' located on the surface of an airfoil. Actually the entire airfoil surface is enveloped by a distribution of pressure and shear stress. Note that the freestream is incident on the airfoil surface at an angle of attack α. Also note that the airfoil could be extruded along z direction to form a wing of finite span as indicated by dotted lines. Flow past an airfoil section is two dimensional whereas that around a finite wing is three dimensional. The integrated effect of pressure and shear stress distribution on the airfoil is the formation of a resultant force and a moment. This is shown in Figure 1.3. Further, the resultant force 'R' could be resolved into a pair of components as shown in Figure 1.4. One pair comprises of lift and drag force, the other pair comprises of normal force (N) and axial force (A). The geometrical relation between these two pair of force components is given by

$$\begin{aligned} L &= N\cos\alpha - A\sin\alpha \\ D &= N\sin\alpha + A\cos\alpha \end{aligned} \tag{1.1}$$

Often the forces and moments are expressed in terms of non dimensional coefficients. For example lift and pitching moment coefficients would be represented as

$$C_L = \frac{L}{q_\infty S},\ \ C_M = \frac{M}{q_\infty Sl} \tag{1.2}$$

When the aerodynamic coefficients are written in capital letters as above they refer to a three dimensional body such as aircraft or finite wing. For a two dimensional body like airfoil the coefficients are written in lower case like c_l, c_m etc. In the above equation $q_\infty = \frac{1}{2}\rho U_\infty^2$ is the dynamic pressure. This is a pressure created by the dynamic state of air. There is another kind of pressure called as static pressure (p_∞) which is developed by virtue of molecular motion and does not depend on macroscopic motion of the medium. The sum of these two pressures gives stagnation pressure. The terms 'S' and 'l' refer to the planform area and characteristic length of the body (in case of the wing it is the wing chord) respectively. For a two dimensional body $S = c \times 1 = c$, where c is the chord of the airfoil and the airfoil is assumed to have unit depth. There is another important non dimensional coefficient called as pressure coefficient which is defined as

$$C_p = \frac{p - p_\infty}{q_\infty} \tag{1.3}$$

1.3.2 Centre of pressure and aerodynamic centre of an airfoil

We have not yet talked about the chord wise position at which the resultant force 'R' should act. It must act at such a position on the body that it represents the effect of all distributed loads acting on the body surface. This point is called the centre of pressure. The pitching moment about the leading edge of the airfoil M_{LE} obtained by integrating the effect of pressure and shear stress distribution acting on the entire airfoil should be identical to that produced by R acting through the centre of pressure. Now R can be resolved into N and A as shown in Figure 1.5. Therefore we can write

$$M_{LE} = -(x_{cp})N \tag{1.4}$$

Refer Figure 1.5 to see the position of forces and moments acting on the airfoil. When the angle of attack of the airfoil is small, the normal force can be closely approximated to the lift force and therefore

$$x_{cp} = -\frac{M_{LE}}{N} \approx -\frac{M_{LE}}{L} \tag{1.5}$$

Further, if we change the reference point for pitching moment to quarter chord point (c/4) we can write

$$M_{LE} = -\frac{c}{4}L + M_{c/4} \tag{1.6}$$

Equation (1.6) can be written in non dimensional form as follows

$$\frac{x_{cp}}{c} = \frac{1}{4} - \frac{c_{m,c/4}}{c_l} \qquad (1.7)$$

It can be shown that for thin symmetric airfoils the centre of pressure is the quarter chord position. That means the second term in the above equation would be zero. This in turn means that about the quarter chord position the pitching moment coefficient for such airfoils is zero and therefore has no dependence on angle of attack. By definition, aerodynamic centre of an airfoil is that point about which pitching moment is independent of angle of attack. Therefore for thin symmetric airfoils that point is located at quarter chord. It can be shown that for thin cambered airfoils too the pitching moment remains constant about the quarter chord point but is non zero.

Example 1.1

For a cambered airfoil at an angle of attack of 5^0 the lift coefficient is 0.95 and pitching moment coefficient about quarter chord=-0.1. Find the location of the centre of pressure. What is the pitching moment coefficient about the leading edge of the airfoil?

Using equation (1.7) we have

$$\frac{x_{cp}}{c} = \frac{1}{4} - \frac{-0.1}{0.95}$$

= 0.355

Assuming that the lift force is nearly equal to the normal force since the angle of attack is small

$$x_{cp} = -\frac{M_{LE}}{N} = -\frac{M_{LE}}{L} = -\frac{\left(M_{LE} / q_\infty c^2\right)}{\left(L / q_\infty c.c\right)} = -\frac{c \times c_{m,LE}}{c_l}$$

Therefore

$$c_{m,LE} = -c_l \times \frac{x_{cp}}{c}$$

= -0.95×0.355

= -0.33725

1.3.3 NACA airfoils

Development of airfoils started from the end of the nineteenth century and still continues to remain a very active field. In the early 1930s, NACA – the forerunner of NASA – embarked on systematic experiments on a series of airfoils which later became well known as NACA airfoils. These are in wide spread use today. Subsequently many more interesting developments have led to new airfoil designs like modern low speed airfoils, supercritical airfoils, diamond shaped supersonic airfoils etc. NACA airfoils are divided into 'four digit', 'five digit' and '6-series laminar flow airfoils'. Common example of one airfoil from each of the above airfoil families are NACA 2412, NACA 23012 and NACA 65-218 respectively. For NACA 2412, the first digit represents maximum camber in hundredths of chord, the second digit is the location of maximum camber from leading edge of airfoil in tenths of chord and the last two digits give the maximum thickness in hundredths of chord. For NACA 23012 airfoil the first digit when multiplied by $\frac{3}{2}$ gives the design lift coefficient in tenths, the next two digits when divided by 2 gives the location of maximum camber along the chord from leading edge in hundredths of chord and the final two digits give the maximum thickness in hundredths of chord. For NACA 65-218 the first digit stands for the series, second gives location of minimum pressure in tenths of chord from leading edge, the third digit is design lift coefficient in tenths and last two digits give maximum thickness in hundredths of chord. There are a large number of other airfoils which are of interest in aerodynamics. They need to be explored by the reader.

1.3.4 Dimensional Analysis: Significance of Reynolds number and Mach Number

Consider flow past two airfoils which vary widely in dimension but are geometrically similar to each other. It can be shown through dimensional analysis that the flow past the two airfoils would be dynamically similar if the following conditions are fulfilled:

1. The streamline patterns past the airfoils are geometrically similar
2. The distribution of $\frac{p}{p_\infty}$, $\frac{u}{U_\infty}$ and other flow field parameters expressed in non dimensional forms are identical when plotted in common non dimensional coordinates
3. The force coefficients are the same

The above conditions would be fulfilled if in addition to the geometric similarity between the two airfoils the similarity parameters between the two flows are identical. There could be several similarity parameters associated with a particular flow situation. Two of the most important ones are Reynolds number (Re_∞) and Mach number (M_∞) which are defined below

$$Re_\infty = \frac{\rho_\infty U_\infty c}{\mu_\infty} \tag{1.8}$$

$$M_\infty = \frac{U_\infty}{a_\infty} \tag{1.9}$$

In the above equations $\rho_\infty, \mu_\infty, a_\infty$ stand for free stream density, coefficient of viscosity and speed of sound in air respectively, all at free stream condition. When the Reynolds number is low the flow is laminar. When it becomes larger it goes through transition and changes to turbulent flow. At lower Reynolds number a large region of the flow surrounding a body is viscous dominated whereas at higher Reynolds number only a thin layer around the body is viscous dominated which is called as the boundary layer. Beyond the boundary layer the flow behaves as if it is inviscid. When the boundary layer is not able to stay attached to the body due to increasing pressure along the body surface due to its geometry (which is called as adverse pressure gradient), it lifts off from the body surface leading to flow separation. The separated flow region is highly viscous.

If the free stream Mach number is lower than one then the flow is subsonic, if greater than one it is supersonic, if it lies between high subsonic and low supersonic it is transonic and if it is very high supersonic then it is called hypersonic. When the flow is considered incompressible the significance of Mach number is lost and it is considered to be zero. In this chapter we are going to predominantly discuss the characteristics and methods of analyzing inviscid incompressible flow.

1.3.5 Streamlines and stream function

Figure 1.6 shows the lift force variation of a symmetric airfoil in incompressible viscous flow as a function of angle of attack. It also shows typical streamline patterns around the airfoil at low and high angle of attack. The streamlines are predominantly attached to the airfoil surface at low angle of attack and at stall angle and beyond the flow separates from the leeward side of the airfoil due to high adverse pressure gradient. The flow shows predominantly inviscid character at low angles of attack and shows viscous effects due to flow separation at stall angle and above. The maximum lift coefficient ($c_{l,max}$) of the airfoil is indicated on the figure. This occurs just before the airfoil stalls and starts losing lift. Stall occurs due to massive flow separation on the leeward side of the airfoil. This can occur typically at an angle of around 12-16^0 depending on the kind of airfoil, freestream Reynolds number etc. If the flow was inviscid in nature, the flow pattern around the airfoil would change with increase in α, but it would never separate from it. Inviscid flow is therefore an idealization which deviates from real viscous flows in its characteristics.

In order to describe the streamlines that we saw in Figure 1.6 it would be useful to define stream function. In two dimensional steady flow a streamline is defined by the following equation

$$\frac{dy}{dx} = \frac{v}{u} \qquad (1.10)$$

The above equation could be integrated to yield an equation of the type $\psi(x, y) = K$. The function ψ is called a stream function. Each streamline has a separate value for the constant K. Difference between two stream function levels $\psi_1 - \psi_2$ gives the mass flux through the gap between two streamlines. Concept of streamline and stream function can be better explained physically by using Figure 1.7. No flow can take place across streamlines because streamlines are tangential to the flow at every point in the flow field. So what we see between two stream function values (ψ_1, ψ_2) is a two dimensional tube which is impermeable to flow in the direction normal to its surface. It is called stream tube. Cartesian velocity components could be expressed as derivatives of stream function as follows

$$u = \frac{\partial \psi}{\partial y}$$

$$v = -\frac{\partial \psi}{\partial x} \qquad (1.11)$$

1.3.6 Angular velocity, vorticity

As a fluid element moves through a flow field along a streamline we also need to pay special attention to the shape and orientation of the element during such movement. This exercise helps us to define a very important quantity in aerodynamics which is called as vorticity. If we look at a two dimensional fluid element in Figure 1.8 at two different instants of time t and t+Δt we can see the rotation and distortion in the element due to the effect of velocity gradients existing in the flow field. We say that the fluid element is undergoing strain under the influence of stresses acting on it. Referring to the figure we can show that the angular velocity of the fluid element is given by

$$\omega_z = \frac{1}{2}\left(\frac{d\theta_1}{dt} + \frac{d\theta_2}{dt}\right) = \frac{1}{2}\left(\frac{\partial v}{\partial x} - \frac{\partial u}{\partial y}\right) \tag{1.12}$$

Note that since the fluid element considered in this case is two dimensional, it has only the z component of angular velocity vector. In general the fluid element would have three dimensional motion and therefore it would have three components of angular velocity. The expression for angular velocity in three dimensional space would be

$$\vec{\omega} = \frac{1}{2}\left[\left(\frac{\partial w}{\partial y} - \frac{\partial v}{\partial x}\right)\hat{i} + \left(\frac{\partial u}{\partial z} - \frac{\partial w}{\partial x}\right)\hat{j} + \left(\frac{\partial v}{\partial x} - \frac{\partial u}{\partial y}\right)\hat{k}\right] \tag{1.13}$$

Vorticity is defined as twice the angular velocity vector as follows. Also vorticity is equal to curl of the velocity vector.

$$\vec{\xi} = 2\vec{\omega} = \nabla \times \vec{V} \tag{1.14}$$

If in a fluid field $\nabla \times \vec{V} = 0$ at all points then it is an irrotational flow. Fluid elements moving in such field do not have any net angular velocity and therefore no vorticity. They are in pure translation. Even if they deform, such deformation follows the following rule $\theta_1 + \theta_2 = 0$. On the contrary, in rotational flow fields $\nabla \times \vec{V} \neq 0$ and the fluid elements have net angular velocity and therefore vorticity.

1.3.7 Circulation

We consider a closed curve C in a fluid flow field. At a directed line segment $\overrightarrow{ds}$ on the curve if fluid velocity is $\vec{V}$ then the circulation along the curve is given by

$$\Gamma = -\oint_C \vec{V}.\overrightarrow{ds} = -\oiint_S \left(\nabla \times \vec{V}\right) \cdot \overrightarrow{dS} \tag{1.15}$$

Note that the curve is traversed in counter clockwise manner. It can be shown that circulation about the curve C is equal to vorticity integrated over any open surface bounded by C. This means that if the flow is irrotational at every point over any surface bounded by C then $\Gamma = 0$. Note that in the above and following integrals both $\overrightarrow{ds}$ and $\overrightarrow{dS}$ are vectors, one is associated with the line integral and the other is associated with the surface integral.

1.3.8 Velocity Potential

In an irrotational flow field we can introduce a scalar function ϕ which would satisfy the following vector identity

$$\vec{\xi} = \nabla \times \vec{V} = \nabla \times \left(\nabla\phi\right) = 0 \tag{1.16}$$

Therefore there exists a scalar function whose gradient at a point is equal to the fluid velocity at that point. From this we can write the expressions for the Cartesian velocity components

$$u = \frac{\partial\phi}{\partial x}, v = \frac{\partial\phi}{\partial y}, w = \frac{\partial\phi}{\partial z} \tag{1.17}$$

1.4 Governing equations of fluid flow

Several models can be used to study the motion of a fluid. Out of all of them one approach seems to be most popular. It considers a fixed finite volume in space through which the fluid is moving. The various fluxes are accounted across the surface of this control volume leading to a set of governing differential equations which account for conservation of mass, momentum, energy, species etc for that control volume. The governing differential equations which emerge from such a model are integral in nature. Differential forms of these equations could be derived by application of Divergence theorem on the integral equations. Figure 1.9 shows such a control volume

- Continuity Equation (Conservation of mass)

Continuity equation in integral form is given as follows:

$$\frac{\partial}{\partial t}\oiiint_{v} \rho dv + \oiint_{S} \rho\vec{V}.\overrightarrow{dS} = 0 \qquad (1.18)$$

In differential form

$$\frac{\partial \rho}{\partial t} + \nabla.\left(\rho\vec{V}\right) = 0 \qquad (1.19)$$

In the above equation t, ρ and v stand for time, density and volume of the control volume. Detailed derivation of the above and the other conservation equations could be studied from any standard reference book. We are just going to physically understand its implication here. Note that the above form of Continuity equation applies to unsteady three dimensional flow of any fluid, compressible or incompressible, viscous or inviscid. If we look at the integral form of the equation, the first term in the equation means time rate of change of mass within control volume and the second term means the rate of net mass outflux from the control volume through its surface. If there is net mass outflux, more mass leaves the control volume than what enters at a given time and therefore the second term becomes positive. In such a situation, the first term becomes equally negative to offset this effect. When the first term becomes negative it means that the mass content of the control volume will decrease with time. This time rate of mass decrease is exactly balanced by the time rate of net mass outflux from the control volume. This ensures mass conservation for the control volume. This concept applies equally well in a differential sense through Equation (1.19).

The first term in the continuity equation is going to vanish if the flow does not change with time. A steady flow remains the same at every instant of time but unsteady flow changes with time. If we assume the flow to be steady then we can drop the first term. The flow field density can be assumed to be constant throughout the field in an incompressible flow until and unless you are heating or cooling it at some place which can locally change its density. We need to remember that such density change is not linked with pressure change which occurs in high speed flow where the medium becomes compressible. In general for incompressible flow the density could be taken outside the divergence operator and therefore we have

$$\nabla.\vec{V} = 0 \qquad (1.20)$$

Now if the flow is irrotational we can further write

$$\nabla.(\nabla\phi) = \nabla^2\phi = 0 \tag{1.21}$$

The above equation is called Laplace equation and is one of the most important equations in aerodynamics and mathematical physics. It falls in the category of elliptic partial differential equation. Analytical solutions of Laplace equation are called harmonic functions. Numerical solution of Laplace equation can be obtained by discretising the terms of the equation in their finite difference form and solving the algebraic equations thus formed under suitable boundary conditions. Another approach which is often taken in aerodynamics is to identify elementary flows which are solutions of Laplace equation and which could be combined judiciously to form new flow solutions of interest. Laplace equation is a linear partial differential equation and therefore two different solutions of it could be combined linearly to form another new solution. If ϕ_1, ϕ_2 are two solutions of Laplace equation, then $k_1\phi_1 + k_2\phi_2$ is a new solution, where k_1, k_2 are constants.

Let us assume that we have a uniform flow along x direction with velocity U_∞. We can show that such a flow is a physically possible incompressible flow and it is irrotational in nature. Therefore we can write the following expressions for the Cartesian velocity components of this flow as follows

$$\frac{\partial \phi}{\partial x} = u = U_\infty$$
$$\frac{\partial \phi}{\partial y} = v \qquad (1.22)$$

By integrating the above equations we get

$$\phi = U_\infty x \qquad (1.23)$$

You can mentally check that it satisfies two dimensional Laplace equation $\frac{\partial^2 x}{\partial x^2} + \frac{\partial^2 y}{\partial y^2} = 0$ .Thus uniform flow is an elementary flow. Note that we can find the equation of the stream function of uniform flow as follows

$$\frac{\partial \psi}{\partial y} = u = U_\infty$$
$$\frac{\partial \psi}{\partial x} = -v = 0 \qquad (1.24)$$

Integrating the above equations we get

$$\psi = U_\infty y \qquad (1.25)$$

Comparing Equations (1.23) and (1.25) we find that velocity potential lines are parallel to y axis and streamlines are parallel to x axis.

We will quickly look at a few other elementary flows which are of importance to us. All of them are solutions of Laplace equation.

a) Source flow

The stream lines and velocity potential lines of source flow are shown in Figure 1.10. The flow emanates from the point source and moves with pure radial velocity. Λ defines the source strength which is equal to the volumetric flow rate from the source per unit depth perpendicular to the plane of the paper. The velocity potential and stream functions are given as follows:

$$\phi = \frac{\Lambda}{2\pi}\ln r$$
$$\psi = \frac{\Lambda}{2\pi}\theta \qquad (1.26)$$

If a sink is placed instead of a source it depletes flow from its neighbourhood by inducing a radial inward velocity. The steamlines point into the sink. Combination of a uniform flow with a source produces a semi infinite body stretching infinitely downstream of the source location and is called as Rankine half body (Figure 1.11(a)). This body has a front stagnation point. When a source and sink of equal magnitude are placed at a finite gap and uniform flow moves past this combination, a closed body known as Rankine oval is formed (Figure 1.11(b)). This body has a front and rear stagnation point. Note that whenever a body surface is simulated using a combination of elementary flows, the body becomes a streamline of the flow and the stream function value there is zero.

b) Doublet flow

When a source and a sink are brought very close to each other and all the while as they are moved closer to each other the product of Λ and the gap between the two (say l) remains constant, as $l \to 0$ a doublet is formed. The stream line pattern is shown in Figure 1.12. Non lifting flow past a circular cylinder is obtained when a uniform source is combined with a doublet. The stream function for this flow is given by

$$\psi = (U_\infty r \sin\theta)\left(1 - \frac{R^2}{r^2}\right) \qquad (1.27)$$

where R is the radius of the circular cylinder and r is the radial location of any point in the flow. The radial and tangential velocities at a point in the flow field are obtained as follows

$$V_r = \frac{1}{r}\frac{\partial\psi}{\partial\theta} = \left(1 - \frac{R^2}{r^2}\right)U_\infty \cos\theta$$
$$V_\theta = -\frac{\partial\psi}{\partial r} = -\left(1 + \frac{R^2}{r^2}\right)U_\infty \sin\theta \qquad (1.28)$$

At the point where the source and sink coexist as $l \to 0$ the absolute magnitudes of both become infinitely large and we have a singularity of strength $(\infty - \infty)$ which is an indeterminate form that can have a finite value. Therefore doublet is a singularity.

c) Vortex flow

Vortex flow develops around a point vortex as shown in Figure 1.13. It is irrotational except at the origin. At the origin the vorticity is infinite. Therefore the origin is a singular point in the flow field. The velocity potential and stream function for vortex flow are as follows

$$\phi = -\frac{\Gamma}{2\pi}\theta$$

$$\psi = \frac{\Gamma}{2\pi}\ln r \qquad (1.29)$$

In the above equations Γ is the circulation around any given circular streamline surrounding the point vortex. If a non lifting flow past a circular cylinder is combined with a point vortex, we have a lifting flow past a circular cylinder. If $\Gamma = 4\pi U_\infty R$ then a single stagnation point is formed on the lower side of the cylinder. If $\Gamma < 4\pi U_\infty R$ two stagnation points are formed which are skewed to the lower half of the cylinder and if $\Gamma > 4\pi U_\infty R$ no stagnation point is formed on the body at all. This flow can be associated closely with lifting flow past a spinning circular cylinder. The lifting force acting on a rotating cylinder is called as Magnus force. In lifting flows the streamlines would be closely packed on the upper surface of the body and more sparsely spaced on the lower side. Close packing of streamlines indicates higher velocities and vice versa. This also means that there is asymmetry in the streamline pattern for lifting flows.

In connection with lifting flows we have a very important theorem called as Kutta-Joukowski theorem which states that lift per unit span of a body is given by

$$L = \rho_\infty U_\infty \Gamma \tag{1.30}$$

Example 1.2

A cylinder with 5 cm diameter with a circulation Γ is placed in free stream with uniform velocity of 5 m/s. Calculate the value of Γ when both the stagnation points coincide on the body. Calculate the lift force acting on the cylinder. Assume density of air ρ=1.22 kg/m^{-3}.

The radial and circumferential velocity components around the lifting cylinder are given by

$$V_r = \frac{1}{r}\frac{\partial\psi}{\partial\theta} = \left(1 - \frac{R^2}{r^2}\right)U_\infty \cos\theta$$

$$V_\theta = -\frac{\partial\psi}{\partial r} = -\left(1 + \frac{R^2}{r^2}\right)U_\infty \sin\theta - \frac{\Gamma}{2\pi r}$$

To locate stagnation points on the body set the above velocities to zero and solve for the coordinates (r,θ). We get by substituting r=R on the body surface

$$\theta = \sin^{-1}\left(-\Gamma/4\pi U_\infty R\right) \text{ and } \pi\text{-}\theta$$

When the two points coincide, the two angles are equal and θ=-π/2 on lower surface. Thus

$$\Gamma = 4\pi U_\infty R$$

Substituting the given numerical values

$$\Gamma = 4\pi \times 5 \times 5/2 \times 10^{-2} = 1.571 \text{ m}^2/\text{s}$$

The lift force per unit span is

$$L = \rho_\infty U_\infty \Gamma = 1.2 \quad \times 5 \times 1.571 = 9.583 \text{N/m}$$

- Momentum Equation (Conservation of Momentum)

Momentum equation in integral form is given as follows

$$\frac{\partial}{\partial t}\oiiint_v \rho\vec{V}dv + \oiint_S \left(\rho\vec{V}.\overrightarrow{dS}\right)\vec{V} = -\oiint_S p\overrightarrow{dS} + \oiiint_v \rho\vec{B}dv + \vec{F}_{viscous} \tag{1.31}$$

In differential form the x component of the equation is written as

$$\frac{\partial(\rho u)}{\partial t} + \nabla.\left(\rho u\vec{V}\right) = -\frac{\partial p}{\partial x} + \rho\overrightarrow{B_x} + \left(\overrightarrow{\overline{F}_x}\right)_{viscous} \tag{1.32}$$

Other components of Momentum equation could be written in a similar manner. We postpone the discussion on the Energy equation for now because we would not need it immediately.

Note that the above form of Momentum equation applies to unsteady three dimensional flow of any viscous fluid, compressible or incompressible. They are more popularly called as Navier Stokes equations. Sometimes the continuity equation is also clubbed with the momentum equations and the combination is called as Navier Stokes equations. The above equation evolves from the application of Newton's second law of motion (Force=time rate of change of momentum) to a fluid control volume or element. All the forces which act on the fluid lie on the right hand side of the equation, they are the cause of fluid motion. They include force due to pressure, body forces (like gravitational force, electromagnetic force etc, which act on the fluid from a distance; indicated by symbol B which stands for body force per unit mass) and viscous force due to viscous stresses. The effect of these forces is to change the momentum of the fluid. The momentum terms are on the left hand side of the equation. They include an unsteady term (first term) and a convective term (second term).

Some drastic simplifications could be applied to this equation to significantly modify it. For example if we have a steady, inviscid flow devoid of body forces, the equation becomes

In integral form

$$\oiint_S \left(\rho\vec{V}.dS\right)\vec{V} = -\oiint_S p\overrightarrow{dS} \tag{1.33}$$

In differential form the x component of the equation is written as

$$\nabla.\left(\rho u\vec{V}\right) = -\frac{\partial p}{\partial x} \tag{1.34}$$

The above form of momentum equation is called as Euler equation and it is used to describe inviscid flow of an incompressible or compressible fluid. Another useful form of Euler equation is

$$dp = -\rho V dV$$
$$\text{where } V = \sqrt{u^2 + v^2 + w^2} \quad (1.35)$$

The above equation relates the change in velocity along a streamline dV to the change in pressure dp along it. When this equation is applied to incompressible flow and is integrated between any two points 1 and 2 along a streamline we have

$$p_1 + \frac{1}{2}\rho V_1^2 = p_2 + \frac{1}{2}\rho V_2^2 \quad (1.36)$$

The above equation holds both for rotational and irrotational flow. If the flow is irrotational, the two points 1 and 2 could be located anywhere in the flow and not necessarily on a streamline. The above equation is known as Bernoulli's equation.

We can now look at an instrument which is used for measuring velocity in the test section of a wind tunnel. It is called as a Pitot Static Tube. Its cross sectional view is given in Figure 1.14. As shown in the figure the probe has a port at its tip and another one on its side which is located some distance downstream of the one at the tip. The port at the tip measures stagnation pressure which is the sum of static and dynamic pressure. The side port measures static pressure. At the tip port the flow stagnates (comes to a halt isentropically, i.e., through a reversible adiabatic process). As a consequence all its dynamic pressure content gets converted into static pressure and an enhanced static pressure is felt by the port which is called as stagnation pressure. At the side port the flow slides tangentially. Therefore that port cannot sense the dynamic pressure. It can only sense static pressure. Let us now see how we could apply Bernoulli's equation to measure air speed with this instrument. If we apply Bernoulli's equation between two points on a steam line such that one is in the free stream and the other is at the front port, we can write

$$p_\infty + \frac{1}{2}\rho U_\infty^2 = p_0 + 0 \tag{1.37}$$

$$\therefore U_\infty = \sqrt{\frac{2(p_0 - p_\infty)}{\rho_\infty}} \tag{1.38}$$

where p_0 is the stagnation pressure.

Example 1.3

In a low speed wind tunnel, we have a settling chamber where the velocity of air is small and the cross section is large. The flow is taken from there through a converging passage where it accelerates before it reaches the test section where the model is kept for testing. If the cross sectional area, velocity and static pressure in the settling chamber and test section are A_S, V_S, p_S and A_T, V_T, p_T respectively find the velocity in the test section in terms of the other parameters.

If we look at our continuity equation in Equation (1.18) and apply it to a control volume stretching from settling chamber to test section we can write

$$\rho_S A_S V_S = \rho_T A_T V_T \tag{1.39}$$

Note that the solid walls of the tunnel would not allow any flow across it and therefore whatever flow gets into the control volume in the settling chamber gets out of it at the test section. Moreover since it is a low speed tunnel the air density is constant. Therefore we have

$$A_S V_S = A_T V_T$$
$$\therefore V_T = \frac{A_S}{A_T} V_S \tag{1.40}$$

Applying Bernoulli's equation between two stations

$$V_T^2 = \frac{2}{\rho}(p_S - p_T) + V_S^2 \tag{1.41}$$

Combining the above two equations we have

$$V_T = \sqrt{\frac{2(p_S - p_T)}{\rho\left[1 - (A_T / A_S)^2\right]}} \tag{1.42}$$

1.5 Thin Airfoil Theory

Since an airfoil is a complicated geometry as compared to simpler ones we have handled in elementary flows, it would be judicious to have a continuous vortex sheet wrapping the whole airfoil surface instead of having discrete singularities. The vortex sheet strength can vary from point to point in such a manner that when combined with uniform flow, the surface of the airfoil will form a streamline of the flow. The strength of this sheet is given by $\gamma = \gamma(s)$, where s is the running coordinate along body surface starting from leading edge. The circulation would be given by

$$\Gamma = \oint_C \gamma ds \tag{1.43}$$

where C is the contour of airfoil surface. When the flow starts on the airfoil, it takes a short while to adjust and then onwards leaves the trailing edge of the airfoil smoothly. When such smooth flow at trailing edge is established we say that Kutta condition is satisfied. In such a situation the vortex sheet strength at trailing edge of airfoil should be zero. There is another important theorem associated with the starting flow past an airfoil which is called as Kelvin's circulation theorem. As the flow over an airfoil starts a vortex sheet leaves the trailing edge of the airfoil. This is called as a starting vortex. Kelvin's circulation theorem states that the sum of the circulation around the starting vortex and that around the airfoil should equate to zero.

The gist of thin airfoil theory is as follows. The airfoil is considered to be thin. Therefore, instead of wrapping the vortex sheet on its surface, the vortex sheet is placed on its camber line. When we look at this picture from a distance, it would appear as through the vortex sheet is approximately lying on the chord line. In this situation, in order to make the camber line a streamline of the flow, the normal component of velocity induced by the vortex sheet at a point on the camber line should exactly balance that due to the free stream which is incident at an angle of attack α (assumed to be small). This idea is shown in Figure 1.15. This concept could be modeled mathematically as follows

$$\frac{1}{2\pi}\int_0^c \frac{\gamma(\xi)d\xi}{x-\xi} = U_\infty\left(\alpha - \frac{dz}{dx}\right) \tag{1.44}$$

The above equation is the fundamental equation of thin airfoil theory. Subject to the satisfaction of Kutta condition at the trailing edge of the airfoil the above equation could be solved using Glauert integrals. Note that the airfoil is in x-z plane. For symmetric airfoils the $\frac{dz}{dx}$ term on right hand side drops out. The following transformation is used to solve the integrals

$$\xi = \frac{c}{2}(1-\cos\theta) \tag{1.45}$$

The solution is simply stated as

$$\gamma(\theta) = 2\alpha U_\infty \frac{(1+\cos\theta)}{\sin\theta} \tag{1.46}$$

Substituting the $\gamma(\theta)$ expression in Equation (1.43) and suitably modifying the limits of integration we can obtain lift per unit span as

$$L = \pi\alpha c \rho_\infty U_\infty^2 \tag{1.47}$$

From this we have

$$c_l = 2\pi\alpha \tag{1.48}$$

Therefore lift curve slope

$$\frac{dc_l}{d\alpha} = 2\pi \tag{1.49}$$

The above equation means that the lift curve slope is 2π rad^{-1} or 0.11 degree^{-1}. Note that since this is an inviscid model, it cannot predict stall or post stall behavior of the airfoil. It predicts that the airfoil continues to generate proportionately higher and higher lift as the angle of attack increases. This is one of the lacunae of inviscid models. Further we have

$$c_{m,le} = -\frac{c_l}{4} \tag{1.50}$$

$$c_{m,c/4} = 0 \tag{1.51}$$

For cambered airfoil we can show

$$c_l = 2\pi\left[\alpha + \frac{1}{\pi}\int_0^\pi \frac{dz}{dx}(\cos\theta_0 - 1)d\theta_0\right] \tag{1.52}$$

$$\frac{dc_l}{d\alpha} = 2\pi \tag{1.53}$$

$$\alpha_{L=0} = -\frac{1}{\pi}\int_0^\pi \frac{dz}{dx}(\cos\theta_0 - 1)d\theta_0 \tag{1.54}$$

$$c_{m,le} = -\left[\frac{c_l}{4} + \frac{\pi}{4}(A_1 - A_2)\right] \tag{1.55}$$

$$c_{m,c/4} = \frac{\pi}{4}(A_2 - A_1) \tag{1.56}$$

$$x_{cp} = \frac{c}{4}\left[1 + \frac{\pi}{c_l}(A_1 - A_2)\right] \tag{1.57}$$

where

$$A_n = \frac{2}{\pi}\int_0^\pi \frac{dz}{dx}\cos n\theta_0 d\theta_0 \tag{1.58}$$

We note a few distinguishing features of the cambered airfoil as compared to symmetric airfoil. Cambered airfoil generates lift at zero angle of attack. It produces non zero pitching moment about quarter chord, but the value remains invariant with respect to α and hence the aerodynamic centre lies at the quarter chord. The centre of pressure is shifted from the quarter chord.

When we try to model lifting flow past airfoils which do not fit well into thin airfoil theory framework (either because the airfoil is thick or the angle of attack is large or the camber is too large) we can look for numerical methods for solution of such problems. The reader could explore the vortex panel method for this purpose.

1.6 Finite Wing Theory

The question to answer in this section before we begin a discussion is that why should the aerodynamic characteristics of a finite wing be different from its airfoil section? The answer is that the finite wing is a three dimensional body which has a finite span. Consequently there is a component of flow on the finite wing in the span wise direction. An airfoil is a section of a wing with theoretically infinite span. Therefore there is no effect of span wise flow on its characteristics. The flow is two dimensional.

We have already said that there is a pressure difference between the lower and upper surfaces of an airfoil. The same applies to the finite wing. However, at the wing edges the high pressure air from the bottom surface tries to run away into the low pressure region on top. This makes the flow curl up at the wing tips. This can be seen in Figure 1.16. The tendency of the flow to leak around the wing tips induces a downward velocity component called downwash which creates an induced angle of attack denoted by α_i . The geometric angle of attack is reduced by this induced angle of attack producing an effective angle of attack given by

$$\alpha_{\text{effective}} = \alpha - \alpha_i \tag{1.59}$$

The effect is not restricted to the reduction in angle of attack alone. Another effect of downwash is to incline the lift force towards the rear direction by α_i . Because of this tilt, a component of the lift force acts along the free stream direction producing an induced drag D_i . See Figure 1.17 to appreciate these issues. The three dimensional flow induced at wing tips alters the pressure distribution on the wing in such a manner that there is a net pressure imbalance in the free stream direction. Therefore induced drag can be treated as a kind of pressure drag. The total drag on a subsonic finite wing is the sum of skin friction drag D_f , pressure drag D_p (which is due to imbalance in pressure acting on front and rear portion of the body when flow is separated in the rear) and induced drag D_i . The sum of the viscous dominated drags, namely skin friction drag and pressure drag is called profile drag. In high speed flows there is an additional drag due to formation of shock waves on the body called as wave drag.

The first theoretical model for flow past a finite wing was proposed by Ludwig Prandtl in his classical lifting line theory. The essence of this theory is to model the finite wing using a horseshoe vortex with a bound vortex portion running along the span of the wing and a pair of free trailing vortices attached at the two ends of the bound vortex and stretching infinitely into the wake of the wing. The total vortex structure is called as a horseshoe vortex. This horseshoe vortex induces a velocity field in its neighborhood which is a fair approximation of the downwash that we observe around a finite wing. Prandtl realized that with a single horseshoe vortex the approximation was not satisfactory. Therefore he proposed a lifting line at the location of the bound vortex along which he superposed infinite number of horseshoe vortices of infinitesimal strength accompanied by a pair of trailing vortices. This gave a very good approximation of the real flow field and the circulation distribution along the wing span was well modeled. Prandtl thus came up with the fundamental equation of his famous lifting line theory

$$\alpha(y_0) = \frac{\Gamma(y_0)}{\pi U_\infty c(y_0)} + \alpha_{L=0}(y_0) + \frac{1}{4\pi U_\infty}\int_{-b/2}^{b/2} \frac{(d\Gamma/dy)}{y_0 - y} \qquad (1.60)$$

The wing spans from –b/2 to b/2, which means its total span is b; $c(y_o)$ is the local sectional chord length of the wing. In physical terms the above equation simply states that the geometric angle of attack is equal to the sum of effective angle plus induced angle of attack. Note that the wing planform is in the x-y plane and y_0 is an arbitrary location on the lifting line. $\Gamma = \Gamma(y)$ is the circulation distribution along the span of the wing.

Prandtl found that with an elliptic circulation distribution (and therefore elliptic lift distribution) given by

$$\Gamma(y) = \Gamma_0\sqrt{1-\left(\frac{2y}{b}\right)^2} \qquad (1.61)$$

where Γ_0 is maximum circulation at mid span, downwash is constant along wing span

$$w(\theta_0) = -\frac{\Gamma_0}{2b} \qquad (1.62)$$

Further

$$L = \rho_\infty U_\infty \Gamma_0 \int_{-b/2}^{b/2}\left(1-\frac{4y^2}{b^2}\right)^{1/2} dy = \rho_\infty U_\infty \Gamma_0 \frac{b}{4}\pi \qquad (1.63)$$

$$\alpha_i = \frac{C_L}{\pi AR} \tag{1.64}$$

$$C_{D,i} = \frac{C_L^2}{\pi AR} \tag{1.65}$$

AR is the aspect ratio of the wing given by

$$AR = \frac{b^2}{S} \tag{1.66}$$

S is the planform area of the wing. For high aspect ratio wings the induced drag $C_{D,i}$ reduces. For elliptic distribution the planform of the wing would have to be elliptic as well.

When the flow past a finite wing of arbitrary planform needs to be obtained an elegant approach would be to numerically model the lifting wing surface with a lattice of horse shoe vortices and finding their strengths such that the wing surface becomes a streamline of the flow when the wing is immersed in uniform flow. This approach is called as vortex lattice method which the reader is encouraged to explore. With this we come to the end of the first chapter.

1.7 Multiple choice questions

1. A pitot static probe measures
a) static pressure
b) stagnation pressure
c) both static and stagnation pressure
d) absolute pressure

2. Aerodynamic forces and moments act at
a) centre of gravity
b) centre of mass
c) centre of pressure
d) aerodynamic centre

3. Lifting flow over an airfoil may be simulated by using a distribution of
a) doublets
b) source and sinks

c) point vortices
d) point vortices and a source

4. Aerodynamic forces arise due to a distribution of
a) shear stress and pressure
b) pressure and surface tension
c) static pressure and dynamic pressure
d) mass and surface stress

5. A finite wing experiences
a) pressure drag only
b) induced drag and wave drag
c) induced drag and viscous drag
d) profile drag only

6. Induced drag is due to
a) wake formation behind airfoil
b) roll up of flow from lower to upper side of a finite wing
c) flow separation on finite wing
d) flow separation on airfoil

7. A safer option during takeoff or landing at an airport is
a) a large aircraft following a small aircraft
b) a formation of small aircrafts following a large aircraft
c) a small aircraft following a large aircraft
d) a series of large aircrafts at close gaps

8. An airfoil can generate positive lift if
a) angle of attack is zero and airfoil is symmetric
b) angle of attack is negative and airfoil is cambered
c) angle of attack is positive and airfoil is cambered
d) angle of attack is zero and airfoil is cambered

9. Laplace equation can be used to solve
a) inviscid incompressible flow
b) viscous incompressible flow
c) viscous compressible flow
d) inviscid compressible flow

10. Two rectangular wings are there, one with aspect ratio=2 (AR2) and the other with aspect ratio 10 (AR10) [Hint: explore how lift curve slope changes with AR]
a) AR2 would generate less lift than AR10 for a small angle of attack
b) AR2 will stall at lower angle of attack than AR10
c) Lift curve slope of AR2 will be greater than AR10
d) Lift curve slope of AR10 will be greater than AR2

11. NACA0012 and NACA2312 airfoils have
a) same thickness distribution
b) same leading edge radius of curvature
c) same zero lift angle of attack
d) same maximum lift coefficient

12. Flow separation on airfoil occurs due to
a) turbulence in the free stream
b) adverse pressure gradient on leeward side
c) favourable pressure gradient on leeward side
d) adverse pressure gradient in the windward side

1.8 Figures

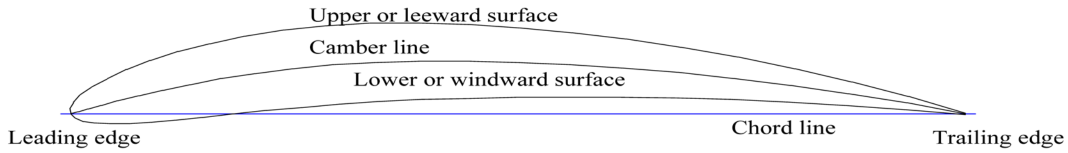

Figure 1.1 Airfoil Nomenclature

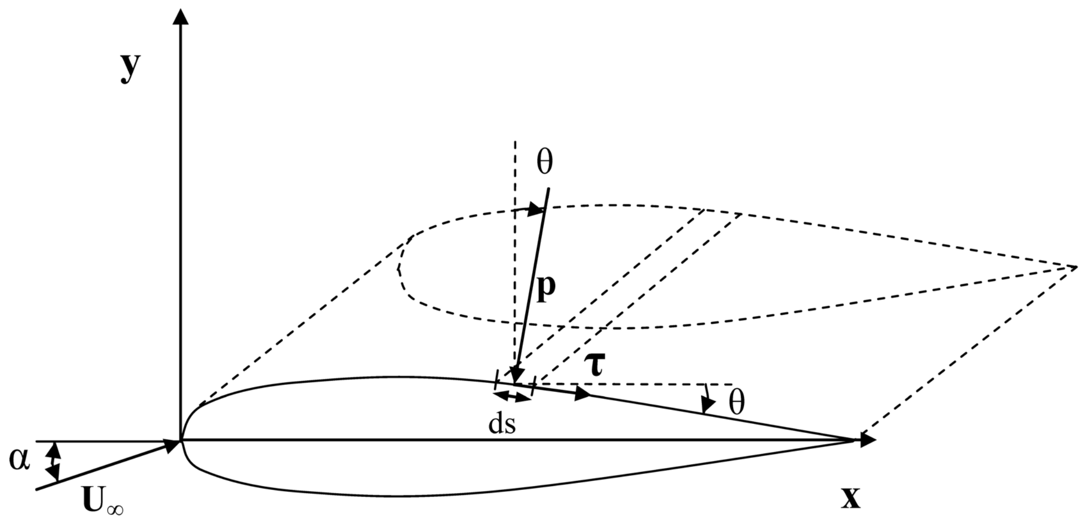

Figure 1.2 Pressure and shear stress acting on a small elemental length on the surface of an airfoil

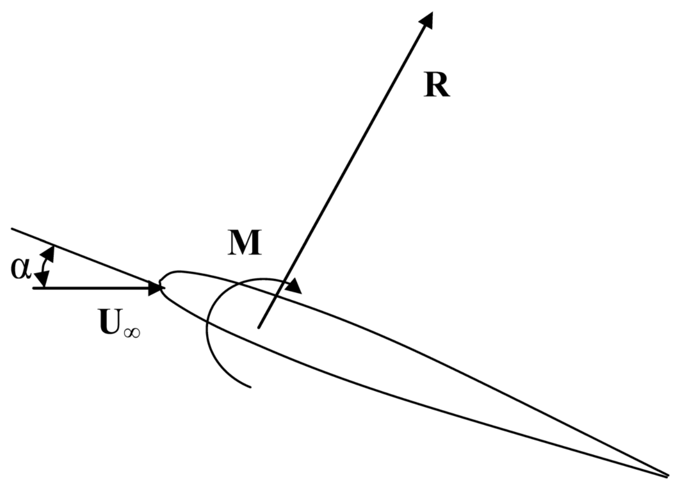

Figure 1.3 Resultant force and moment acting on an airfoil

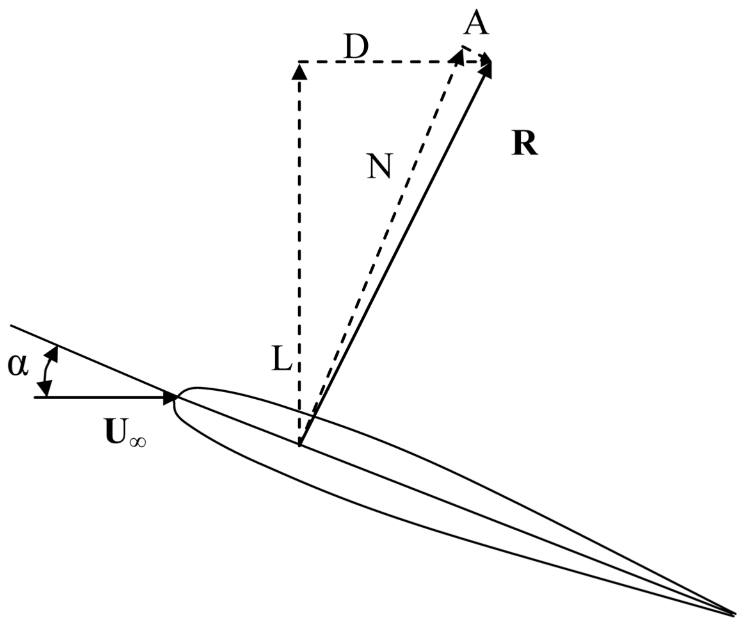

Figure 1.4 Resolving the resultant force into a pair of components

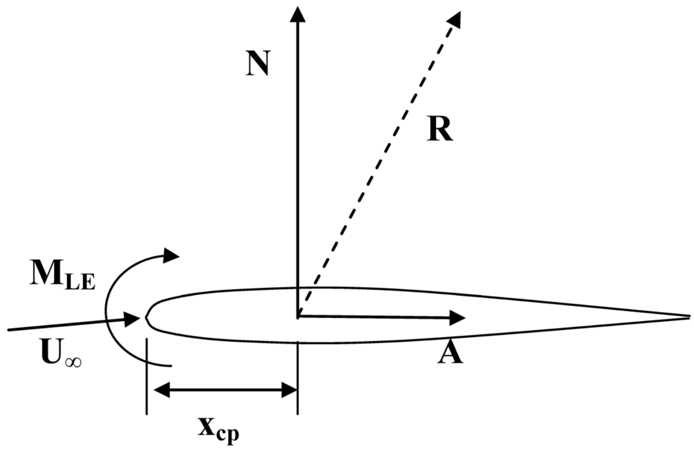

Figure 1.5 Centre of pressure for an airfoil

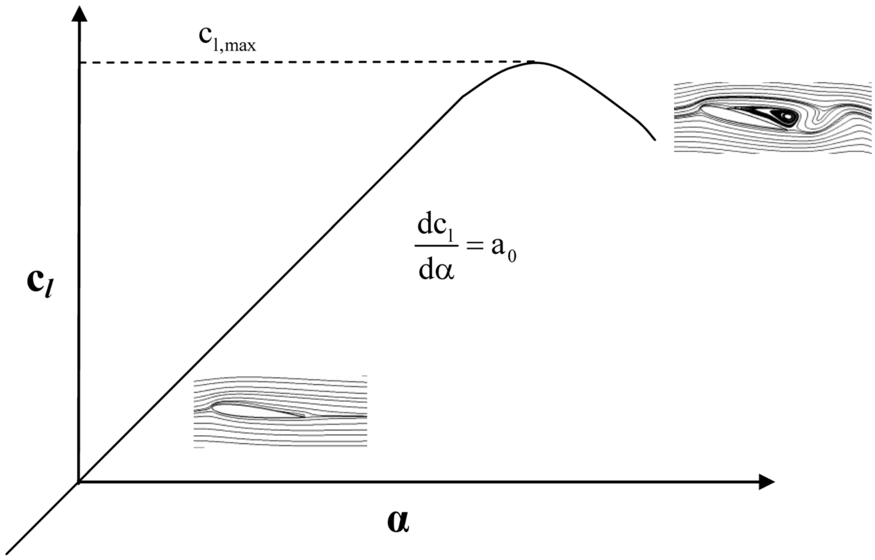

Figure 1.6 Lift coefficient versus angle of attack for a symmetric airfoil along with streamlines at low and high angles of attack

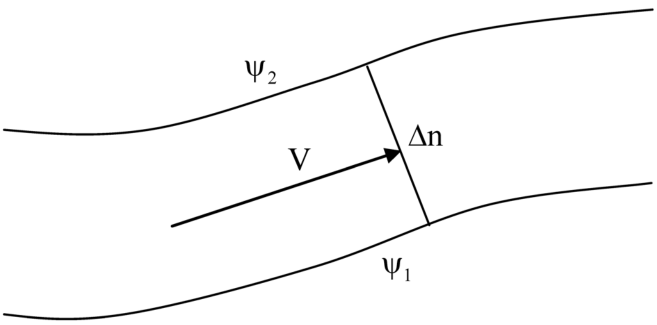

Figure 1.7 Steamlines in a flow field

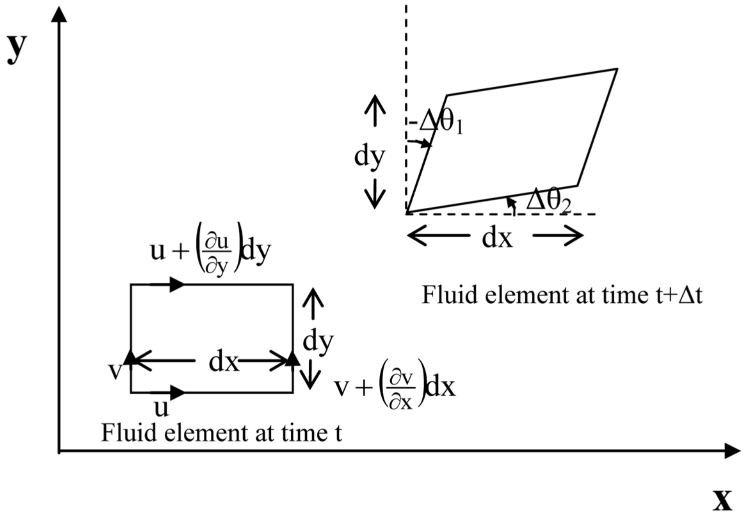

Figure 1.8 Rotation and distortion of a fluid element

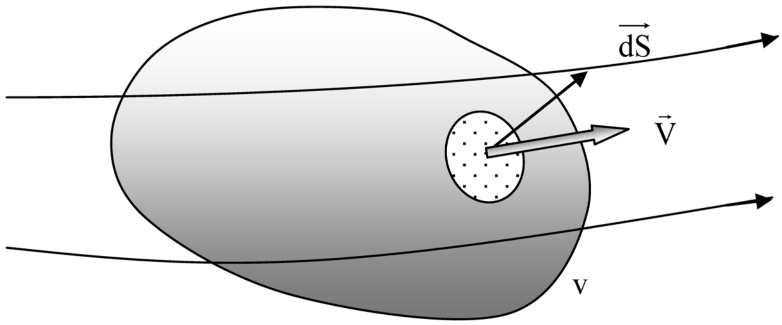

Figure 1.9 Control volume for conservation equations

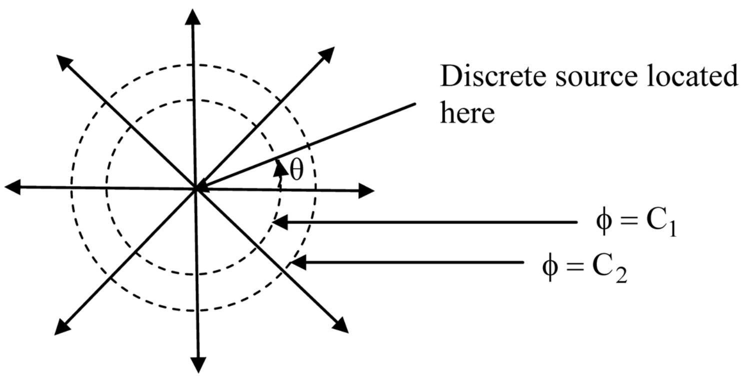

Figure 1.10 Streamline pattern for source flow

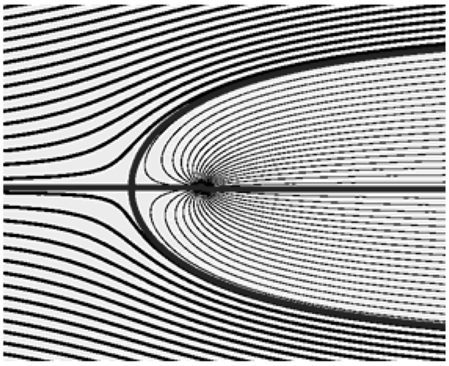
(a)

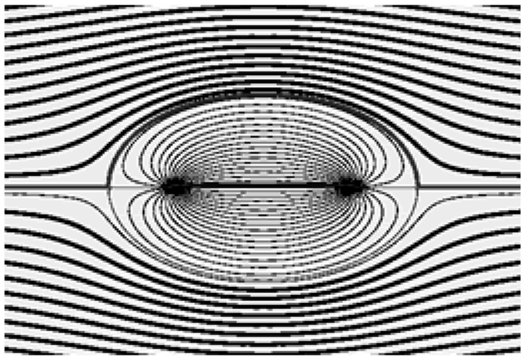
(b)

Figure 1.11 Streamline pattern around (a) Rankine half body (b) Rankine oval

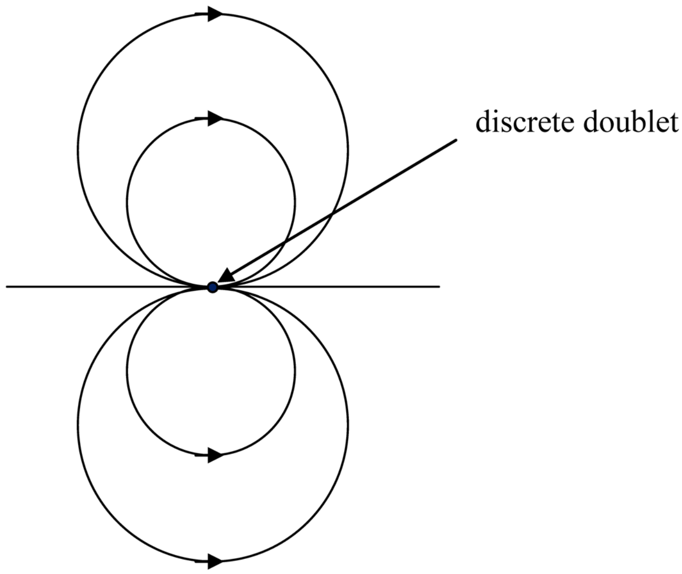

Figure 1.12 Streamline pattern around Doublet

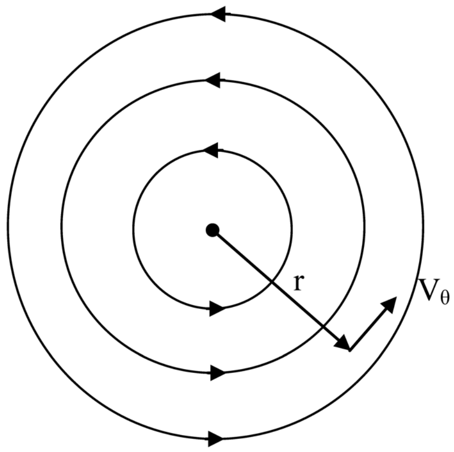

Figure 1.13 Streamline pattern around point vortex

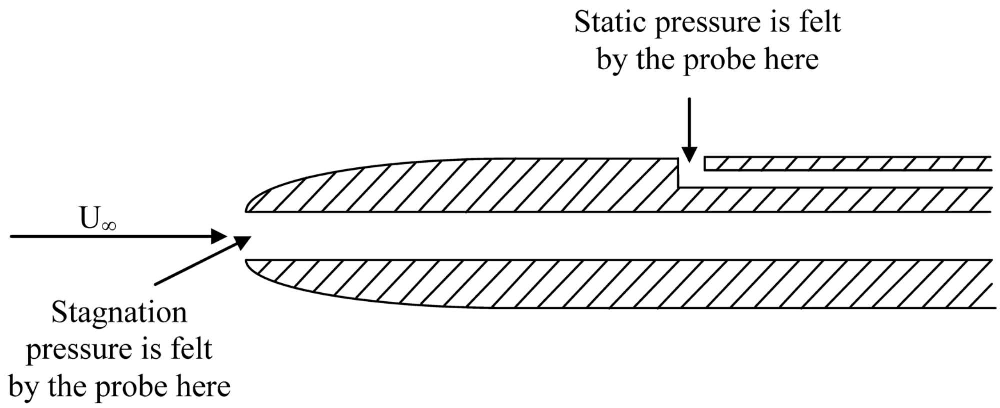

Figure 1.14 Schematic diagram of Pitot Static Tube

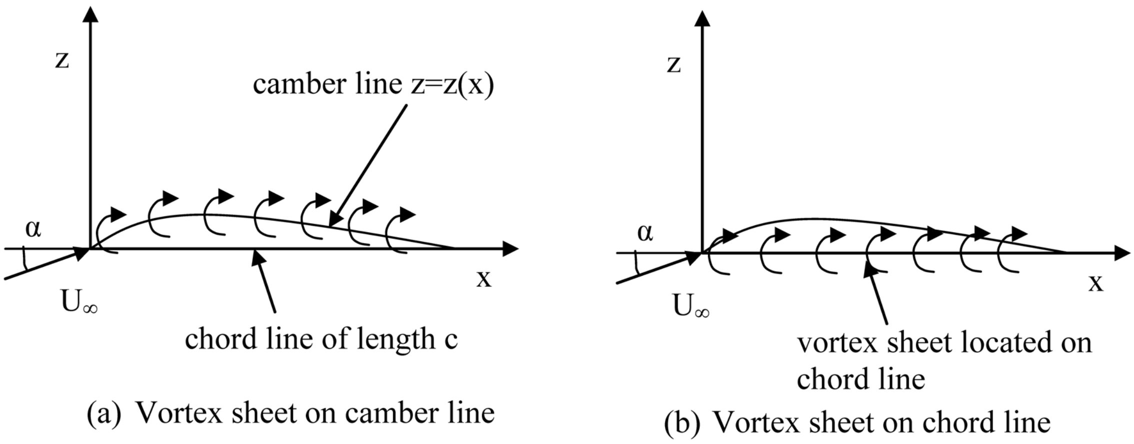

Figure 1.15 Vortex sheet in thin airfoil theory model

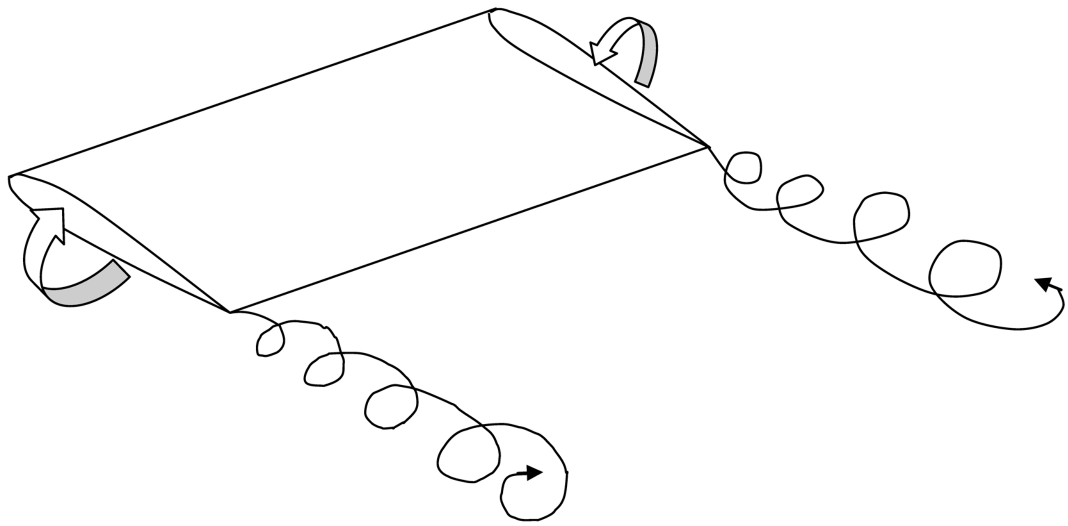

Figure 1.16 Formation of wing tip vortices in a finite aspect ratio wing

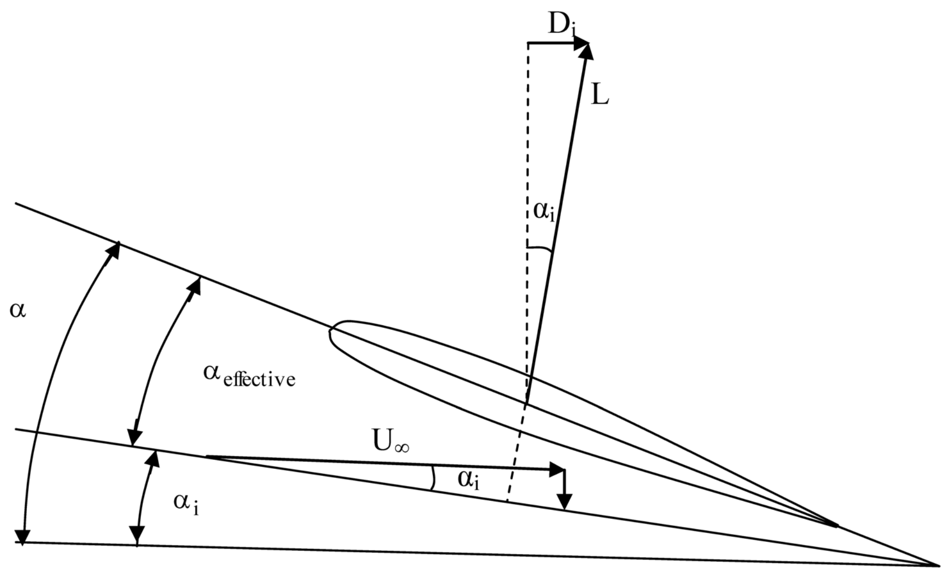

Figure 1.17 Effect of downwash over a section of finite wing

2 Fundamentals of Inviscid Compressible Flow

2.1 Introduction

In this chapter we would discuss about important features of inviscid compressible flow. The flow becomes compressible as the flow speed increases. As M_∞ exceeds 0.3 the flow starts to exhibit compressibility. The concept of compressibility can be explained using a simple example. Consider a small element of fluid of volume v. The pressure exerted on the surface of the element by the neighboring fluid is p. If the pressure acting on the element is now increased by an infinitesimal amount dp the volume of the element will be correspondingly compressed by the amount dv. The change would be accompanied by a negative sign because it is a reduction. The compressibility of the fluid can then be defined as

$$\tau = -\frac{1}{v}\frac{dv}{dp} \tag{2.1}$$

The corresponding change in density of the fluid is given by

$$d\rho = \rho\tau dp \tag{2.2}$$

For a given change in pressure, dp, due to the flow, Equation 2.2 shows that the resulting change in density will be small for liquids due to their low values of compressibility, and large for gases due to their high values of compressibility. Therefore, for the flow of liquids, relatively large pressure gradients can create high velocities without much change in density. Hence, such flows are usually assumed to be incompressible, where density is constant. However, for the flow of gases moderate to strong pressure gradients lead to substantial changes in the density. Such flows are called as compressible flows.

There are various flow regimes in compressible flow, namely subsonic compressible flow, transonic flow, supersonic and hypersonic flow. For example, in the case of flow past an airfoil, as long as the free stream Mach number is around 0.7, the flow remains subsonic over the entire airfoil. It needs to be remembered that the local Mach number over the airfoil varies as a function of its shape and could well exceed the freestream Mach number in regions of high acceleration especially on the upper surface. If M_∞ is subsonic but sufficiently close to 1.0, then there could well be a local pocket of supersonic flow on the upper surface of the airfoil. This pocket of supersonic flow is terminated with a shock wave, which is a discontinuous surface formed within the flow field across which many of the flow properties change abruptly. This kind of flow is called a transonic flow. If M_∞ is increased to slightly above unity, this shock pattern will move to the trailing edge of the airfoil, and a second shock wave appears upstream of the leading edge. This second shock wave is called the bow shock because of its shape and it is formed ahead of the airfoil and has no contact with the airfoil surface. This kind of bow shock is also formed around bodies with a blunted nose in supersonic and hypersonic flow regimes.

Essentially, shocks are formed in a supersonic flow whenever it encounters an obstruction. A flowfield where Mach number is uniformly greater than 1 everywhere is defined as supersonic. For values of $M_\infty > 5$, the shock wave is formed very close to the surface, and the flowfield between the shock and the body becomes very hot. The heat could be enough to dissociate or even ionize the gas. The flow regime $M_\infty > 5$ is called as hypersonic flow.

The kinetic energy contained in unit mass of a high speed flowing gas, namely, $V^2/2$ is substantial. As the flow moves externally or internally over or through various objects, the local velocity, and hence local kinetic energy, changes rapidly by large extents. In contrast to low speed or incompressible flow, these energy changes are substantial enough to strongly interact with other properties of the flow. Therefore energy concepts and consequently thermodynamics plays a major role in the study and understanding of compressible flow. The governing equations of compressible flow are continuity equation (1.18), momentum equation (1.31) and energy equation as given below in its integral form.

$$\oiiint_V \dot{q}\rho dv - \oiint_S p\vec{V}.\vec{dS} + \oiiint_V \rho(\vec{f}.\vec{V})dv = \oiiint_V \frac{\partial}{\partial t}\left[\rho\left(e+\frac{V^2}{2}\right)\right]dv + \oiint_S \rho\left(e+\frac{V^2}{2}\right)\vec{V}.d\vec{S} \qquad (2.3)$$

In the above equation 'e' stands for internal energy. The first term on the left hand side of the above equation stands for the amount of heat added to control volume, the second term stands for work done by pressure and third term stands for work done by body forces on the control volume. Therefore the summation of second and third terms stands for rate of work done on the fluid inside the control volume. The first term on the right hand side stands for time rate of change of energy inside the control volume due to possible variation of flowfield variables within the control volume and second terms stands for net rate of flow of energy across the control surface. The three conservation equations mentioned above in conjunction with the equation of state of the gas (Equation (2.4)) and the thermodynamic relation (Equation (2.5)) are sufficient tools to analyze inviscid compressible flows of an equilibrium gas. The gas is assumed to be a perfect gas here. A perfect gas is one in which intermolecular forces are neglected. If the property of the gas varies grossly from that of a perfect gas then a suitable equation of state would need to be used.

$$p = \rho RT \qquad (2.4)$$

$$e=e(T,v) \qquad (2.5)$$

In Equation (2.5), 'T' stands for temperature and 'v' for specific volume of the gas. For problems involving a perfect gas at relatively low temperatures, it is possible to also assume a calorically perfect gas. A calorically perfect gas is defined as a perfect gas with constant specific heats. In such a gas specific heat at constant pressure c_p , specific heat at constant volume c_v and also their ratio, namely, $\gamma = c_p/c_v$, are all constant. Many of the equations of compressible aerodynamics are derived based on the assumption of a calorically perfect medium.

2.2 One Dimensional Flow Equations: Isentropic flow, stagnation condition, Normal Shock

Certain simple compressible flows can be classified as one dimensional compressible flow. Flow past a normal shock wave is one such flow. Normal shock is a thin layer formed perpendicular to the flow direction across which there is almost discontinuous jump of certain flow and thermodynamic properties like static pressure, temperature, density, velocity, entropy, etc. Again, certain properties like stagnation temperature or stagnation enthalpy remain conserved. It is a very strong pressure wave which is formed when a large number of weaker pressure waves agglomerate. Normal shocks can form near the nose region of blunt objects, inside converging-diverging flow passages etc. When a shock is tilted to the flow direction it is called an oblique shock. The flow field across such a shock is two dimensional.

Consider the flow through a one-dimensional control volume as represented in Figure 2.1. There may be a normal shock wave, a sound wave which is an infinitesimally weak pressure wave or there may be some heat addition or removal occurring in this control volume. In all the above cases, the flow properties change as a function of location as the gas flows through the region. Let us assume that to the left of this region, the flowfield velocity, pressure, temperature, density, and internal energy are given by $u_1, p_1, T_1, \rho_1, e_1$ respectively. Similarly, $u_2, p_2, T_2, \rho_2, e_2$ are the properties on the right hand side of the control volume. In general, we have a flow property ϕ_1 at the inlet and ϕ_2 at the outlet of this control volume. If the cross sectional area of the control volume is A, it is the same on the left and right faces of the control volume. By applying the steady Continuity equation to the flow we get

$$\rho_1 u_1 = \rho_2 u_2 \qquad (2.6)$$

Applying steady, inviscid momentum equation with no body forces (Equation 1.31) to the flow we get

$$p_1 + \rho_1 u_1^2 = p_2 + \rho_2 u_2^2 \tag{2.7}$$

For flow with zero body force and heat addition the energy equation is expressed as follows:

$$\frac{\dot{Q}_{cv}}{\rho_1 u_1 A} + p_1 v_1 + e_1 + \frac{u_1^2}{2} = p_2 v_2 + e_2 + \frac{u_2^2}{2} \tag{2.8a}$$

or

$$\dot{q} + h_1 + \frac{u_1^2}{2} = h_2 + \frac{u_2^2}{2} \tag{2.8b}$$

In the above equations '$\dot{q}$' stands for heat per unit mass, 'v' stands for specific volume, 'h' for enthalpy respectively. If there is no volumetric heat transfer then Equation (2.8b) reduces to

$$h_{01} = h_{02} \tag{2.8c}$$

In the above equation h_0 stands for stagnation enthalpy at a respective station. Equation (2.8c) is basically a statement of conservation of stagnation enthalpy. By applying the above conservation equations to a one dimensional control volume containing a sound wave, an expression for speed of sound, 'a', could be derived as

$$a = \sqrt{\left(\frac{\partial p}{\partial \rho}\right)_s} \tag{2.9}$$

where the subscript 's' stands for isentropic condition. Note that sound wave is an infinitesimally weak pressure wave. Therefore flow properties across such a wave would be perturbed infinitesimally. Flow would thus behave isentropically. Using the following isentropic relation

$$pv^{\gamma} = C \tag{2.10}$$

the above expression for ‘a’ reduces to

$$a = \sqrt{\frac{\gamma p}{\rho}} \tag{2.11}$$

Further by using the equation of state (Equation 2.4) the expression becomes

$$a = \sqrt{\gamma RT} \tag{2.12}$$

Speed of sound at standard sea level conditions is around 340 m/s. The Mach number of a flow is defined using ‘a’ as follows

$$M = \frac{V}{a} \tag{2.13}$$

where ‘V’ is the velocity of the gas. When M<1 it is subsonic flow, when M=1 it is sonic flow and when M>1 it is supersonic flow respectively.

Consider a point P in a flow field. Let us suppose that a fluid element instantaneously crosses this point with velocity V. Its Mach number, pressure and temperature are M, p and T respectively. Imagine that the fluid element is adiabatically (i.e., without heat addition or removal) slowed down to M=1 (if it was originally traveling at supersonic Mach number) or speeded up to M=1 (if it was originally traveling at subsonic Mach number). As this process takes place the temperature of the fluid element would change. The new temperature of the fluid element at this state would be defined as T^*. The speed of sound at this temperature would be defined according to Equation (2.12) as

$$a^* = \sqrt{\gamma RT^*} \tag{2.14}$$

Using the above equation we can define a characteristic Mach number given by

$$M^* = \frac{V}{a^*} \tag{2.15}$$

We can think of another hypothetical state change. As the fluid element crosses point P with velocity V we imagine slowing down the fluid element to zero velocity isentropically (i.e. by keeping the overall entropy unaltered; which is possible if the process is reversible adiabatic). The pressure and temperature that the fluid element would attain after coming to halt is called as stagnation pressure, denoted by p_0 and stagnation temperature, denoted by T_0 respectively. Static pressure (p) and static temperature (T) are manifestations of random microscopic molecular motion within the fluid element whereas the stagnation values are comprised of a static as well as a dynamic component. The dynamic component comes from the macroscopic kinetic energy of the molecules in the direction of flow.

If we now look back at Equation (2.8c) and assume that the gas is calorically perfect, then we can write the equation as follows

$$c_p T_1 + \frac{u_1^2}{2} = c_p T_2 + \frac{u_2^2}{2} \tag{2.16}$$

Note that the above form of energy equation is valid for adiabatic flows. We remove the subscripts for station 1 and imagine that the gas reaches stagnation condition at station 2. Then we can write the above equation as

$$c_p T + \frac{u^2}{2} = c_p T_0 \tag{2.17}$$

It is to be noted from the above equation that when defining stagnation temperature the flow needs to be adiabatic but not necessarily isentropic. The definition for T_0 in terms of static temperature and Mach number can be worked out as follows

$$\frac{T_0}{T} = 1 + \frac{u^2}{2c_p T} = 1 + \frac{u^2}{2\gamma RT/(\gamma - 1)} = 1 + \frac{\gamma - 1}{2} M^2 \tag{2.18}$$

Now if the state 2 was reached by the gas through an isentropic process instead of an adiabatic one, we could use the following relation to relate stagnation pressure and stagnation density with stagnation temperature.

$$\frac{p_0}{p} = \left(\frac{\rho_0}{\rho}\right)^{\gamma} = \left(\frac{T_0}{T}\right)^{\frac{\gamma}{(\gamma-1)}} \tag{2.19}$$

Therefore by using Equation (2.18) and (2.19) we get

$$\frac{p_0}{p} = \left(1 + \frac{\gamma - 1}{2} M^2\right)^{\frac{\gamma}{(\gamma-1)}} \tag{2.20}$$

$$\frac{\rho_0}{\rho} = \left(1 + \frac{\gamma - 1}{2} M^2\right)^{\frac{1}{(\gamma-1)}} \tag{2.21}$$

It is to be noted from the above two equations that when defining stagnation pressure and density the flow needs to be isentropic.

We recall that Equations (2.6), (2.7) and (2.8c) are the governing continuity, momentum and energy equations for the case of a normal shock placed inside the one dimensional control volume. For a normal shock the relation between upstream and downstream quantities, namely Mach number, density, velocity, pressure, temperature and enthalpy are given in the following equations. The reader should be able to derive them independently.

$$M_2^2 = \frac{1+\left[(\gamma-1)/2\right]M_1^2}{\gamma M_1^2-(\gamma-1)/2} \tag{2.22}$$

$$\frac{\rho_2}{\rho_1} = \frac{u_1}{u_2} = \frac{(\gamma+1)M_1^2}{2+(\gamma-1)M_1^2} \tag{2.23}$$

$$\frac{p_2}{p_1} = 1+\frac{2\gamma}{\gamma+1}\left(M_1^2-1\right) \tag{2.24}$$

$$\frac{T_2}{T_1} = \frac{h_2}{h_1} = \left[1+\frac{2\gamma}{\gamma+1}\left(M_1^2-1\right)\right]\left[\frac{2+(\gamma-1)M_1^2}{(\gamma+1)M_1^2}\right] \tag{2.25}$$

Not that the temperature ratio (Equation (2.25)) is obtained by using the equation of state and the pressure and density ratio equations. The entropy change can be calculated using the following equation

$$s_2 - s_1 = c_p \ln\frac{T_2}{T_1} - R\ln\frac{p_2}{p_1} \tag{2.26}$$

Equations (2.24) and (2.25) are to be substituted in the above equation. Note that entropy would increase across a normal shock.

The above results emphasize the fluid dynamic nature of shock waves. Essentially a shock wave can be considered as a thermodynamic device which compresses the medium. Therefore the changes across a shock could be expressed purely in terms of thermodynamic variables. This is through the Hugonoit equation

$$e_2 - e_1 = \frac{p_1+p_2}{2}\left(v_1 - v_2\right) \tag{2.27}$$

In the above equation v stands for specific volume. The above equation states that the internal energy increase across a shock is equal to the average pressure across the shock times the reduction in specific volume.

Example 2.1

A normal shock wave is formed in air where upstream Mach number is 2 and upstream temperature, pressure and density are 300 K, 1 atm (i.e., 1 atmospheric pressure, which is approximately $1.01\times10^5\,\mathrm{N/m^2}$) and $1.2\,\mathrm{kg/m^3}$ respectively. Calculate Mach number, velocity, static temperature, static pressure, stagnation temperature and stagnation pressure downstream of the shock. Assume $\gamma = 1.4$.

$$M_2^2 = \frac{1+0.2\times 4}{1.4\times 4-0.2} = 0.333$$

$$\Rightarrow M_2 = 0.58$$

$$a_1 = \sqrt{1.4\times 287\times 300} = 347.2\text{m/s}$$

$$u_1 = M_1 \times a_1 = 2\times 347.2 = 694.4\text{m/s}$$

$$p_2 = p_1\left(1+\frac{2\times 1.4}{2.4}(4-1)\right) = 4.5\text{atm}$$

$$\frac{\rho_2}{\rho_1} = \frac{2.4\times 4}{2+0.4\times 4} = 2.67$$

$$\frac{T_2}{T_1} = \frac{p_2}{p_1}\times\frac{\rho_1}{\rho_2} = \frac{4.5}{2.67} = 1.6875$$

$$\Rightarrow T_2 = 506.3\text{K}$$

$$u_2 = M_2 \times a_2 = 0.58\times\sqrt{1.4\times 287\times 506.3} = 261.5 \text{ m/s}$$

$$\frac{T_{0,2}}{T_2} = 1+\frac{\gamma-1}{2}M_2^2$$

$$\Rightarrow T_{0,2} = 506.3 \times (1 + 0.2 \times 0.333) = 540\text{K}$$

$$\frac{p_{0,2}}{p_2} = \left(1 + \frac{\gamma - 1}{2} M_2^2\right)^{\frac{\gamma}{\gamma-1}}$$

$$\Rightarrow p_{0,2} = 4.5 \times (1 + 0.2 \times 0.333)^{3.5} = 5.64\text{atm}$$

It is interesting to find out the loss in stagnation pressure across the shock. Upstream stagnation pressure is

$$p_{0,1} = (1 + 0.2 \times 4)^{3.5} = 7.82\text{atm}$$

Therefore loss in stagnation pressure across the normal shock=2.18atm. Stagnation temperature is conserved across the shock.

2.3 Quasi One Dimensional Flow: Nozzle and diffuser flow

Consider the flow through a two dimensional duct whose cross section changes gradually along its length. The flow is considered to be quasi one dimensional because the rate of change of cross sectional area with axial distance is small. We can imagine a control volume slightly modified from Figure 2.1, where inlet area on the left is 'A' and outlet area on the right is slightly larger than 'A'. The upper and lower surfaces are slightly curved to match the areas at inlet and outlet. Therefore, the flow properties can be considered to be varying only along the flow direction and not along the cross flow direction. Let us consider that the station 1 is the inlet station and station 2 is the outlet station of the duct. The governing equations for quasi one dimensional steady adiabatic flow without body forces are as follows

$$\rho_1 u_1 A_1 = \rho_2 u_2 A_2 \tag{2.28}$$

$$p_1 A_1 + \rho_1 u_1^2 A_1 + \int_{A_1}^{A_2} p\,dA = p_2 A_2 + \rho_2 u_2^2 A_2 \tag{2.29}$$

$$h_{01} = h_{02} \tag{2.30}$$

Note that there is an integral term on the left hand side of Equation (2.29) which represents the pressure force on the sides of the control surface. Note that if the control volume was a one-dimensional one then this term would vanish because the pressure force would be acting on equal areas on both stations leading to net zero unbalanced force along the axial direction and there would be no cross sectional area term in Equation (2.29), thereby reducing it to Equation (2.7).

It would be interesting to look at the differential form of the above equations. We would begin with the momentum equation in its differential form. Let us imagine that the control volume shrinks to an infinitesimal axial length dx. This leads to a control volume with cross sectional area A at station 1 and cross sectional area (A+dA) at station 2 respectively. The flow properties undergo infinitesimal change across the control volume due to this infinitesimal change in cross sectional area, e.g., pressure changes from p to p+dp. When Equation (2.29) is applied to the above infinitesimal control volume we get

$$pA + \rho u^2 A + pdA = (p + dp)(A + dA) + (\rho + d\rho)(u + du)^2 (A + dA) \quad (2.31)$$

From Equation (2.28) the differential form of continuity equation is written as

$$d(\rho u A) = 0 \quad (2.32)$$

By neglecting the second order terms involving products of differentials in Equation (2.31) and using Equation (2.32) we get

$$dp = -\rho u du \quad (2.33)$$

Equation (2.33) is the differential form of Euler's equation. The reader is urged to explore the differential form of energy equation.

Now one-dimensional isentropic flow in a stream tube with slowly varying cross-section A can be investigated with the conservation equations given above. Another way of representing the differential form of continuity equation is as follows

$$\frac{d\rho}{\rho} + \frac{du}{u} + \frac{dA}{A} = 0 \quad (2.34)$$

The differential of the density in the above equation can be eliminated with the aid of Equation (2.33) assuming isentropic flow as follows:

$$-udu = \frac{dp}{\rho} = \left(\frac{dp}{d\rho}\right)\left(\frac{d\rho}{\rho}\right) = a^2 \frac{d\rho}{\rho} \quad (2.35a)$$

Therefore

$$\frac{d\rho}{\rho} = -M^2 \frac{du}{u} \quad (2.35b)$$

Substituting the above relation in Equation (2.34) we get the area velocity relation as follows

$$\frac{dA}{A} = (M^2 - 1)\frac{du}{u} \tag{2.36}$$

Based on the above equation three cases can be distinguished:

1. Subsonic flow ($M < 1$)
   The velocity increases with decreasing cross section.
2. Supersonic flow ($M > 1$)
   The velocity increases with increasing cross section.
3. Sonic flow ($M = 1$)
   Sonic velocity can only be attained in the stream tube, if dA vanishes locally.

According to this result supersonic flow can only be generated, if the stream tube has a convergent-divergent distribution of the cross section (de Laval nozzle). The cross section with minimum area, where the local velocity is equal to the speed of sound, is called critical cross section or throat.

Another very important relation for compressible flow through converging-diverging nozzle is given by the area Mach number relation as follows

$$\left(\frac{A}{A^*}\right)^2 = \frac{1}{M^2}\left[\frac{2}{\gamma+1}\left(1+\frac{\gamma-1}{2}M^2\right)\right]^{\frac{\gamma+1}{\gamma-1}} \tag{2.37}$$

Equation (2.37) tells us that Mach number at any section of the nozzle is a function of the area ratio, namely (A/A*), which is the ratio of the local duct area to the sonic throat area. As is evident from the above equation , 'A' must be greater than or at least equal to A*, the case where A < A* is physically not possible in an isentropic flow. Also, the equation would yield two values of M corresponding to a given area ratio, one would be subsonic and another supersonic value.

Consider a convergent-divergent nozzle, as sketched in Figure 2.2. Area ratio at the inlet of the nozzle is very large because it is connected to a large reservoir at pressure and temperature p_o and temperature T_o, respectively. Because of the large inlet area ratio, Mach number is approximately zero at the reservoir end. Hence the pressure and temperature at the reservoir are essentially stagnation values. Furthermore, we assume that the nozzle expands the flow isentropically to supersonic speeds at its exit. For the given nozzle, there is only one possible isentropic solution for supersonic flow, and Equation (2.37) defines it. In the convergent portion of the nozzle, the subsonic flow is accelerated, with the subsonic Mach number defined for local value of (A/A*). At the throat, where the throat area A=A*, M=1. In the divergent portion of the nozzle, the flow expands to supersonic condition, with the supersonic value of Mach number defined for local value of (A/A*). At a given Mach number the Equations (2.18), (2.20) and (2.21) can be applied to find out the variation of static temperature, pressure and density with respect to the corresponding stagnation values respectively along the length of the nozzle. For making such a plot area ratio has to be defined as a function of axial length from the reservoir end of the nozzle. The temperature and pressure ratios at the sonic throat is given by the following equations which are obtained by substituting M=1 and γ=1.4 in Equations (2.18) and (2.20) respectively.

$$\frac{T}{T_0} = 0.833 \tag{2.38}$$

$$\frac{p}{p_0} = 0.528 \tag{2.39}$$

When sonic flow exists at the throat of the nozzle, it is said to be choked. In this condition, the nozzle passes maximum possible mass flow rate. If the back pressure is reduced with an intention of increasing the mass flow rate, the nozzle does not respond to it. The mass flow rate seems to have frozen to a value given by the following equation

$$\dot{m} = \frac{p_0 A^*}{\sqrt{T_0}}\sqrt{\frac{\gamma}{R}\left(\frac{2}{\gamma+1}\right)^{\frac{\gamma+1}{\gamma-1}}} \tag{2.40}$$

The pressure that exists in the ambient atmosphere or in a downstream reservoir where the nozzle discharges is called as back pressure. If the pressure at the exit plane of the nozzle is above the back pressure, the flow further expands to adjust with that back pressure. Expansion fan is formed at the lip of the nozzle. If the back pressure is gradually increased beyond the value for which isentropic supersonic flow exists in the nozzle, oblique shocks are formed at nozzle exit. With further increase in back pressure a normal shock forms at the nozzle exit and gradually moves upstream into the diverging portion of the nozzle. When sufficiently large back pressure exists, the flow may even become entirely subsonic throughout the length of the nozzle because the pressure difference across the nozzle is not large enough for the flow to reach sonic condition at the throat. The flow through the nozzle stops when upstream reservoir pressure is equal to back pressure. Therefore, a whole range of flow conditions can be created within the nozzle by controlling the back pressure, or more generally by controlling the difference between upstream reservoir pressure and back pressure.

2.4 Oblique shocks and Expansion waves

The normal shock wave is a special case of a more general family of oblique waves that occur in supersonic flow. When a supersonic flow moves across a concave corner, it can be considered to be 'turned into itself' and this leads to the formation of an oblique shock. It is intuitively understood that an oblique shock is weaker than a normal one and therefore the change in flow and thermodynamic properties are less drastic across it. A concave corner is often called as a compression corner because it compresses the flow (Figure 2.3). When a supersonic flow moves across a convex corner the flow expands and leads to formation of an expansion fan (Figure 2.4). The flow expands isentropically through this fan which is called as Prandtl-Meyer expansion fan. Across the expansion fan Mach number increases and the pressure, temperature and density decrease. Stagnation values remain constant.

Let us consider a weak source of sound moving through air at supersonic speed. The sound waves emitted by the source form spheres which expand with time. For ease of visualisation in a two dimensional sense we can consider circular wave fronts expanding with time. These wave fronts form a disturbance envelope. The tangent to the family of circles is defined as a Mach wave. Mach wave makes an angle μ with the direction of propagation of the sound source which is expressed in terms of its Mach number as follows

$$\mu = \sin^{-1}\left(\frac{1}{M}\right) \tag{2.41}$$

If the disturbance is stronger than a weak source of sound, e.g., a wedge shaped body moving at supersonic speed, then the wave front becomes stronger than a Mach wave. The strong disturbances agglomerate to form an oblique shock wave. Mach wave is therefore a limiting case of an infinitely weak oblique shock.

Since an oblique shock is inclined to the flow direction, the flow across it is two dimensional in nature. For ease of analysis, usually tangential and normal directions to the shock are considered. Two important facts about oblique shocks are:

a) Tangential component of the flow velocity and the associated momentum is preserved across an oblique shock wave. Therefore, the velocity and momentum change is entirely limited to the normal direction.

b) The governing relations for normal shock waves could be used to obtain change in flow properties across an oblique shock by replacing the upstream Mach number by the normal component of upstream Mach number. The normal component of Mach number is given as

$$M_{n1} = M_1 \sin\beta \tag{2.42}$$

Where β is called as wave angle. It is defined as the angle made by the oblique shock with horizontal direction. For an oblique shock the normal component of downstream Mach number is given by

$$M_{n2}^2 = \frac{1+\left[(\gamma-1)/2\right]M_{n1}^2}{\gamma M_{n1}^2-(\gamma-1)/2} \tag{2.43}$$

Pressure ratio is given by

$$\frac{p_2}{p_1} = 1+\frac{2\gamma}{\gamma+1}\left(M_{n1}^2-1\right) \tag{2.44}$$

Similarly the other relations for oblique shock wave may be written by using normal component of Mach number. An important relation that connects the compression angle θ, wave angle β and free stream Mach number M is called as $\theta-\beta-M$ relation which is given as follows

$$\tan\theta = 2\cot\beta\left[\frac{M_1^2\sin^2\beta-1}{M_1^2(\gamma+\cos 2\beta)+2}\right] \quad (2.45)$$

For any given M_1 there is a maximum deflection angle θ_m. If the physical geometry is such that $\theta > \theta_m$, then no solution exists for a straight oblique shock wave. Instead, the shock will be curved and detached upstream from the compression corner. For any given $\theta < \theta_m$, there are two values of θ predicted by the $\theta-\beta-M$ relation. The large value is called the strong shock solution and the small value as weak shock solution. In nature, usually the weak shock solution is observed.

In the case of an expansion fan a Prandtl-Meyer function is defined as follows

$$\nu(M) = \sqrt{\frac{\gamma+1}{\gamma-1}}\tan^{-1}\sqrt{\frac{\gamma-1}{\gamma+1}(M^2-1)} - \tan^{-1}\sqrt{M^2-1} \quad (2.46)$$

By substituting the upstream Mach number M_1 in the above relation we obtain $\nu(M_1)$. From the geometry of the problem, the expansion angle $\Delta\theta$ can be obtained as

$$\Delta\theta = \theta_2 - \theta_1 \quad (2.47)$$

where θ_1 and θ_2 are the inclinations of the surfaces in regions 1 and 2 respectively. The expansion angle is defined in terms of the change of Prandtl-Meyer function as follows

$$\Delta\theta = \nu(M_2) - \nu(M_1) \quad (2.48)$$

From the above equation the value of $\nu(M_2)$ is obtained. Equation (2.46) can be used to iteratively calculate M_2. Alternatively, Prandtl-Meyer function tables can be used to obtain M_2. Since the expansion process is isentropic, the properties in region 2 can be calculated using isentropic relations.

Example 2.2

A supersonic flow at Mach number=2, temperature=300K, pressure=1atm and density=$1.2\text{kg}/\text{m}^3$ approaches a compression corner. An attached oblique shock with wave angle=45° is formed at the corner. Find the normal Mach numbers upstream and downstream of the shock. Also find M_2, p_2, p_{02}. Assume γ=1.4.

From $\theta-\beta-M$ relation

$$\tan\theta = 2\left[\frac{4\times\left(\sqrt{2}\right)^2-1}{4(1.4+0)+2}\right] = 0.263$$

$$\Rightarrow \theta = 14.74°$$

$$M_{n1} = M_1 \sin\beta = \sqrt{2}$$

$$M_{n2}^2 = \frac{1+0.2\times\left(\sqrt{2}\right)^2}{1.4\times 2-0.2} = 0.538$$

$$M_2 = \frac{M_{n2}}{\sin(\beta-\theta)} = 1.45$$

$$p_2 = 1\times\left(1+\frac{2\times 1.4}{2.4}(2-1)\right) = 2.17\text{atm}$$

$$\frac{p_{0,2}}{p_2} = \left(1+\frac{\gamma-1}{2}M_2^2\right)^{\frac{\gamma}{\gamma-1}}$$

$$\Rightarrow p_{0,2} = 2.17\times(1+0.2\times 1.45^2)^{3.5} = 7.41\text{atm}$$

Note that the stagnation pressure would be the same as in Example 2.1, i.e., $p_{0,1} = 7.82$. Therefore loss in stagnation pressure across oblique shock is 0.41 atm, which is far less than that for a normal shock. Therefore it reiterates the fact that an oblique shock is a weaker shock than normal shock.

2.5 Linearised Theory: Compressible flow past thin airfoil

When an irrotational, inviscid, compressible flow is considered the continuity, momentum and energy equations simplify to a single governing equation in one dependent variable, namely, the velocity potential Φ, the gradient of which gives the velocity vector. The velocity potential equation is given as

$$\left(1-\frac{\Phi_x^2}{a^2}\right)\Phi_{xx} + \left(1-\frac{\Phi_y^2}{a^2}\right)\Phi_{yy} + \left(1-\frac{\Phi_z^2}{a^2}\right)\Phi_{zz} - \frac{2\Phi_x\Phi_y}{a^2}\Phi_{xy} - \frac{2\Phi_x\Phi_z}{a^2}\Phi_{xz} - \frac{2\Phi_y\Phi_z}{a^2}\Phi_{yz} = 0 \quad (2.49)$$

The velocity potential in the above equation is linked to the velocity components as

$$u = \frac{\partial\Phi}{\partial x},\ v = \frac{\partial\Phi}{\partial y},\ w = \frac{\partial\Phi}{\partial z} \quad (2.50)$$

In Equation (2.49) 'a' is variable. From energy equation assuming that stagnation enthalpy is constant in the flow an expression for 'a' is obtained which is given below

$$a^2 = a_0^2 - \frac{\gamma - 1}{2}\left(\Phi_x^2 + \Phi_y^2 + \Phi_z^2\right) \tag{2.51}$$

where $a_0 = \sqrt{\gamma R T_0}$. For a given flow the Equations (2.49) and (2.51) are used to solve for the velocity potential in the flow field under specified boundary conditions. Once velocity potential is obtained, the velocity components can be obtained from Equation (2.50). The velocity magnitude is obtained at each point using

$$V = \sqrt{u^2 + v^2 + w^2} \tag{2.52}$$

'a' is calculated from Equation (2.51). The ratio of V and 'a' gives Mach number and therefore the values of temperature, pressure, density etc in the field. Therefore once Φ is calculated the properties of the entire flow field are known. The Equations (2.49) and (2.51) in combination forms a nonlinear partial differential equation. It can be applied to any irrotational isentropic flow irrespective of the Mach number, namely, for subsonic, transonic, supersonic or hypersonic flow. For incompressible flow $a \rightarrow \infty$ and hence Equation (2.49) yields the Laplace equation. The total velocity potential Φ can be segregated into two components, one due to the free stream flow and the other due to perturbation velocity potential ϕ as follows

$$\Phi(x, y, z) = V_\infty x + \phi(x, y, z) \tag{2.53}$$

Assuming small perturbations, Equation (2.49) reduces to a much simpler form which is applicable to subsonic and supersonic flows but not to transonic and hypersonic flows. This is called the linearised small-perturbation velocity potential equation which is given as follows

$$\left(1 - M_\infty^2\right)\frac{\partial^2\phi}{\partial x^2} + \frac{\partial^2\phi}{\partial y^2} + \frac{\partial^2\phi}{\partial z^2} = 0 \tag{2.54}$$

This equation can be used to solve flow past a thin airfoil or a flat plate at small angle of attack or any slender body at small angle of attack in subsonic and supersonic flow. For subsonic compressible flow an expression for pressure coefficient at a point on the body surface can be derived using the above tools which is called as Prandtl Glauert rule

$$C_p = \frac{C_{p_0}}{\sqrt{1 - M_\infty^2}} \tag{2.55}$$

where C_{p_0} is the pressure coefficient at that point on the body for incompressible flow. Application of this rule leads to Prandtl Glauert compressibility correction. Corrected lift and moment coefficients are expressed as

$$C_l = \frac{C_{l_0}}{\sqrt{1 - M_\infty^2}} \tag{2.56}$$

$$C_m = \frac{C_{m_0}}{\sqrt{1 - M_\infty^2}} \tag{2.57}$$

For supersonic flow the expression for pressure coefficient is given as follows

$$C_p = \frac{2\theta}{\sqrt{1 - M_\infty^2}} \tag{2.58}$$

where θ is the local surface inclination. The above discussion dealt with linearised subsonic and supersonic flow and the associated compressibility corrections. Unfortunately this linearised analysis does not hold well in transonic and hypersonic regime. The transonic regime spans over $0.8 \le M_\infty \le 1.2$. Consider a thin airfoil in transonic flow regime. When we are at the subsonic end of this regime, for a 'critical free stream Mach number', at one point on the upper surface of the airfoil M=1 is reached. As the free stream Mach number exceeds this limit gradually a pocket of supersonic flow develops on the upper side of the airfoil and it terminates with a shock. With increase in free stream Mach number as the terminating shock gets stronger, the wave drag acting on the airfoil increases. Also the strong shock induces the flow to separate from the airfoil surface due to strong adverse pressure gradient acting on the boundary layer formed on the airfoil surface. This is called as shock boundary layer interaction and is essentially an inviscid viscous interaction phenomenon. This leads to a significant drag increase on the airfoil. Typically the drag can increase by a factor of 10. The value of M_∞ for which this sudden large increase in drag starts is defined as 'drag-divergence Mach number'. Efficient flying vehicles in transonic Mach number regime use thin airfoil and swept wing design in order to reduce wave drag and increase critical Mach number. Another two design features which are used in all contemporary transonic flying vehicles are 'area rule' and 'supercritical airfoil'. The reader is encouraged to explore these issues through further reading.

2.6 Hypersonic flow

Hypersonic aerodynamics is associated with flows at high Mach numbers, usually higher than 5. Like transonic flow, hypersonic flow is also highly non linear in nature. These flows are found to occur on reusable space shuttles during atmospheric reentry, long range ballistic missiles which fly through the outer extent of the atmosphere at hypersonic speeds, on rockets at high altitudes, etc. Flow characteristics change significantly as Mach number becomes large which are briefly discussed below. Shock waves are formed closer to the body surface than at supersonic speeds. The thin flow region formed between the shock and the body surface is called as a thin shock layer. Viscous dissipation within this layer is very large at hypersonic speed which leads to excessive heating of the flow. This heat also gets transferred to the body surface. All the three modes of heat transfer, namely, radiative, convective and conductive may play a role because of excessively high temperatures ranging to tens of thousands Kelvin. The body must be protected by a heat shield which is often ablative in nature. Due to enormous heating, flow density reduces and consequently boundary layer thickens. Therefore the displacement effect on the outer inviscid flow becomes stronger and in turn leads to substantial modification of pressure distribution on the body. This affects the forces and moments acting on the body and consequently its stability. At high temperatures the flow becomes chemically reacting, therefore altering its thermodynamic characteristics. The calorically perfect gas assumption which is widely used for supersonic flow breaks down due to the dependence of specific heats (c_p and c_v) on both pressure and temperature in hypersonic condition. Also, complex chemical reactions occur at the body surface if it is coated with an ablative layer for cooling purposes. Since the flow is a t a high speed a fluid particle in the free stream crosses the vehicle length within a very short time. If chemical reactions get completed within this short transit time, they are said to be equilibrium chemical reactions, if not, they are said to be non equilibrium chemical reactions. The equilibrium or non-equilibrium nature of chemical reactions can alter the flow characteristics. Very often hypersonic vehicles have a blunt nose. Since the θ is very large near the nose, close to 90^o, a curved detached shock called as a bow shock is formed. The portion of the shock near the nose of the body is normal. The distance between the nose of the body and the normal portion of the shock is called as shock stand off distance. Since the shock is formed away from the body surface the enormous heat formation across the shock wave at hypersonic speeds is largely carried away by the flow and a lesser amount of heat reaches the surface, which is desirable. Due to the highly curved bow shock the shock angle changes from point to point along its length and consequently leads to varying entropy change across it. This leads to the formation of a layer of strong entropy gradient in the flow behind the shock and this layer convects downstream and wets the body surface. This layer of strong entropy gradient carries considerable amount of vorticity which interacts strongly with the boundary layer and alters its characteristics.

Some interesting facts about hypersonic flows are revealed if we try to impose the limit of $M_\infty \to \infty$ in exact relations for normal and oblique shocks. For example if we apply this limit to the exact normal shock relations we have the following findings:

$$\lim_{M_1 \to \infty} M_2 = \sqrt{\frac{\gamma - 1}{2\gamma}} = 0.378 \text{ assuming } \gamma = 1.4 \tag{2.59}$$

$$\lim_{M_1 \to \infty} \frac{\rho_2}{\rho_1} = \frac{\gamma + 1}{\gamma - 1} = 6 \tag{2.60}$$

The above relations show that under the limiting condition the downstream Mach number and density ratio attain finite values. However some other ratios can become infinitely large. Similarly if we apply this limiting condition to the $\theta - \beta - M$ relation for flow past an oblique shock wave we can show that

$$\lim_{M_1 \to \infty} \beta = \frac{\gamma + 1}{2} = 1.2\theta \tag{2.61}$$

assuming $\gamma = 1.4$ and θ is small. The above relation reiterates the fact that the shock layer is thin at hypersonic speed.

2.7 Multiple choice questions

1. When a moving fluid particle is brought to rest adiabatically.
   a) p_0 and T_0 are both conserved
   b) p_0 is conserved but T_0 is not conserved
   c) p_0 is not conserved but T_0 is conserved
   d) p_0 and T_0 are both not conserved

2. For choked flow through a converging diverging nozzle a normal shock can form at
   a) throat
   b) converging portion
   c) diverging portion
   d) nozzle exit

3. The entropy rise across a normal shock wave is a function of
   a) p_1 and p_2

b) p_{01} and p_{02}
c) T_{01} and T_{02}
d) none of the above

4. In a supersonic flow disturbances can propagate
a) upstream
b) downstream
c) in all possible directions
d) none of the above

5. For supersonic flow at freestream Mach number M_∞ past a two dimensional wedge of semi wedge angle θ the shock can get detached if
a) M_∞ increases and θ increases
b) M_∞ decreases and θ decreases
c) M_∞ decreases and θ increases
d) M_∞ increases and θ decreases

6. The Mach number downstream of an expansion corner could be calculated using the
a) deflection angle, γ and static temperature of upstream flow
b) deflection angle and γ
c) upstream Mach number
d) deflection angle alone

7. A supercritical airfoil has
a) higher wave drag
b) higher critical Reynolds number
c) higher critical Mach number
d) higher drag divergence Mach number

8. Pressure coefficient on the surface of an airfoil at M_∞ =0.7 could be calculated using
a) Bernoulli's theorem
b) Area rule
c) Prandtl-Glauert rule
d) none of the above

9. For subsonic compressible flow past an airfoil at M_∞=0.7, the pressure coefficient at a point on the airfoil would be
a) 40% higher than incompressible pressure coefficient
b) 40% lower than incompressible pressure coefficient
c) 30 % higher than incompressible pressure coefficient
d) 30 % lower than incompressible pressure coefficient

2.8 Figures

Figure 2.1 Control volume for one dimensional flow

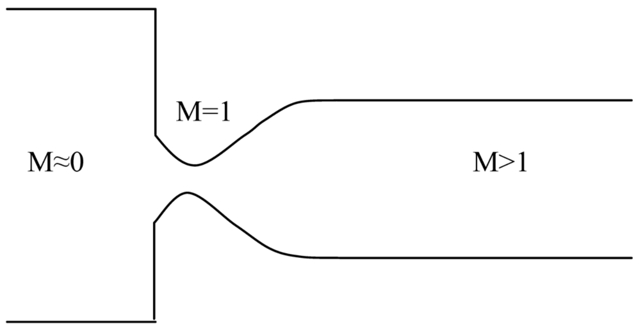

Figure 2.2 Convergent divergent nozzle

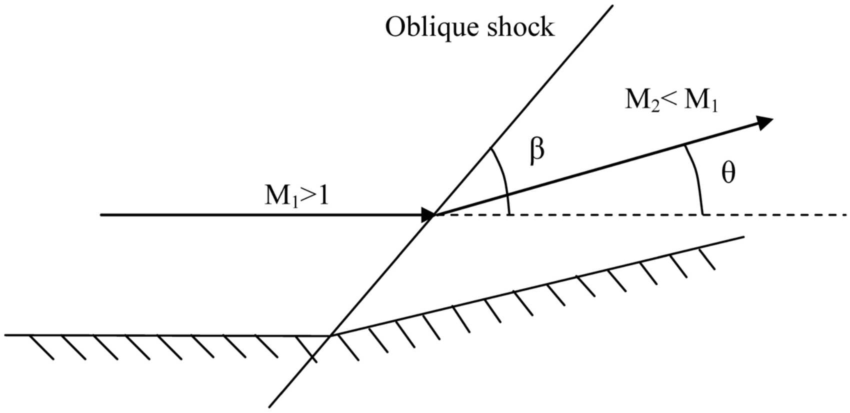

Figure 2.3 Oblique shock wave occurring at a compression corner in supersonic flow

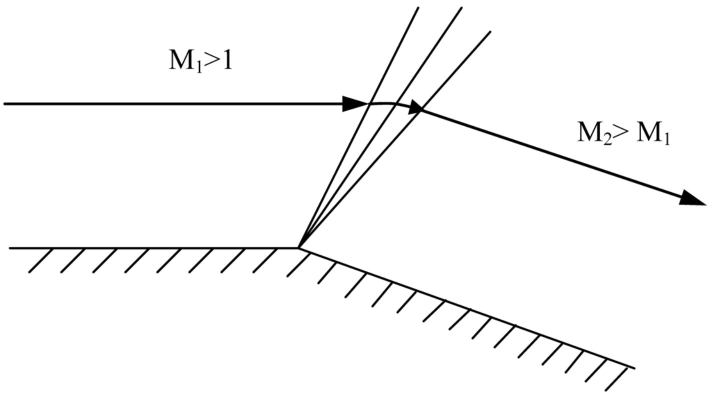

Figure 2.4 Expansion fan occurring at a convex corner in supersonic flow

3 Fundamentals of Viscous Flow

3.1 Introduction

In the preceding chapters the emphasis was on developing theories for inviscid flows over different speed regimes. Viscous term was included in the Momentum equation (Equations (1.31)–(1.32)) for a general viscous flow situation, but its effect was not considered while developing the inviscid flow theories subsequently. However, all real fluids are, in general, viscous having characteristics which are completely different from that of inviscid fluids. In viscous flow, the additional normal and shear stresses due to viscosity must be taken into account in addition to stress due to fluid pressure. The unsteady compressible Navier Stokes equations describe the motion of compressible, viscous fluids with body forces, heat transfer and possible unsteady effects. These equations may be solved in their full or reduced form as demanded by a given flow problem. For all the flow problems that would be discussed in the present chapter we are going to assume viscous incompressible constant property flow without body forces, heat transfer and unsteady effects.

Two viscous flow problems are described in the following section for which exact solution exists. Viscous stress and strain rate would be discussed in the context of these exact solutions. Subsequently the boundary layer concept would be introduced. Boundary layer flows occur at relatively high Reynolds numbers for flows or portion of flows which are attached to the body surface. Viscous flows, like inviscid ones, can occur both internally through ducts, nozzles, diffusers, combustors, etc and externally past flat plate, airfoil, wing, fuselage, aircraft, missile, rocket etc.

3.2 Exact Viscous Flow Solutions

3.2.1 Two Dimensional Poiseuille Flow

In this case a two dimensional incompressible constant temperature viscous flow moves along +x direction between two fixed parallel plates by virtue of the pressure gradient which exists along the flow direction (Figure (3.1)). The flow extends to infinity in both directions along the x axis. This implies that the velocity does not change along x direction, it is only a function of y. Since the streamlines are parallel, the component of velocity along y direction, v=0. Governing equation for the viscous flow can be derived from the equilibrium condition of a small fluid element located in the flow shown in Figure 3.2. The only forces acting on a the fluid element of cross sectional area Δx Δy and of unit depth are the pressure force and the frictional force due to shear stress. The equation of motion for the fluid element in the x-direction is given by

$$p\Delta y-\left(p+\frac{\partial p}{\partial x}\Delta x\right)\Delta y-\tau_{yx}\Delta x+\left(\tau_{yx}+\frac{\partial \tau_{yx}}{\partial y}\Delta y\right)\Delta x=0 \tag{3.1}$$

where τ_{yx} is the viscous shear stress acting on the bottom side of the fluid element . We now need to spend a little time on developing an expression for shear stress in terms of the flow properties. In contrast to solid mechanics where stress is proportional to strain, in fluid mechanics or aerodynamics stress is proportional to time rate of strain. Referring to Figure 1.8 the strain of a fluid element in x-y plane (due to velocity gradients existing in the fluid field) is given as

$$\text{Strain}=\Delta\theta_2-\Delta\theta_1 \tag{3.2}$$

Assuming that the incremental angles in the above equation are small, time rate of strain in x-y plane is equal to

$$\varepsilon_{xy}=\frac{\partial v}{\partial x}+\frac{\partial u}{\partial y} \tag{3.3}$$

Similarly strain rates in other planes can be defined. The constant of proportionality which links stress with strain rate is the viscosity coefficient μ. Hence shear stress is given as

$$\tau_{xy}=\mu\left(\frac{\partial v}{\partial x}+\frac{\partial u}{\partial y}\right) \tag{3.4}$$

Considering zero net moment acting on a three dimensional fluid element under equilibrium as shown in Figure 3.3 we get

$$\tau_{xy} = \tau_{yx} \tag{3.5}$$

Shear stresses acting on the other planes are defined as

$$\tau_{yz} = \tau_{zy} = \mu\left(\frac{\partial w}{\partial y} + \frac{\partial v}{\partial z}\right) \tag{3.6a}$$

$$\tau_{zx} = \tau_{xz} = \mu\left(\frac{\partial u}{\partial z} + \frac{\partial w}{\partial x}\right) \tag{3.6b}$$

Viscous normal stresses act in addition to pressure in the normal direction. These stresses act to compress or expand the fluid element, thereby changing its volume. Normal stresses could be very large inside a shock wave. However, usually, they are small in magnitude compared to the shear stresses. Expressions for three components of normal stresses are

$$\tau_{xx} = \lambda\left(\nabla.\vec{V}\right) + 2\mu\frac{\partial u}{\partial x} \tag{3.7a}$$

$$\tau_{yy} = \lambda\left(\nabla.\vec{V}\right) + 2\mu\frac{\partial v}{\partial y} \tag{3.7b}$$

$$\tau_{zz} = \lambda\left(\nabla.\vec{V}\right) + 2\mu\frac{\partial w}{\partial z} \tag{3.7c}$$

For incompressible flow the divergence term drops off from the Equations (3.7a)-(3.7c). For compressible flows, where the divergence term is non zero in general, the value used for bulk coefficient λ is $-\frac{2}{3}\mu$ according to Stokes hypothesis. This much familiarity with viscous stresses is enough for us to continue with the study of two dimensional Poiseuille flow problem.

In this problem, there is no pressure variation along the y direction because there is no net flow in that direction and the hydrostatic pressure variation is negligible in gaseous media, therefore p=p(x). To emphasize this we write Equation (3.1) as

$$-\left(\frac{dp}{dx}\right)\Delta x\Delta y + \frac{\partial \tau_{yx}}{\partial y}\Delta x\Delta y = 0$$

Then using Equations (3.4) and (3.5) and recalling that v and its derivatives are zero throughout the flow field, we have $\tau_{yx} = \mu\frac{\partial u}{\partial y}$. Also, due to the same reason, there is no net shear force acting on the left and right faces of the control volume shown in Figure 3.2. Therefore, the above equation gives

$$-\left(\frac{dp}{dx}\right)+\mu\frac{\partial^2 u}{\partial y^2}=0$$

$$\mu\frac{\partial^2 u}{\partial y^2}=\left(\frac{dp}{dx}\right)$$

Integrating with respect to y

$$\mu\frac{\partial u}{\partial y}=\left(\frac{dp}{dx}\right)y+C_1$$

Integrating again with respect to y

$$\mu u=\left(\frac{dp}{dx}\right)\frac{y^2}{2}+C_1 y+C_2$$

$$u=\frac{y^2}{2\mu}\left(\frac{dp}{dx}\right)+\frac{C_1}{\mu y}+\frac{C_2}{\mu}$$

$$=\frac{1}{2\mu}\left(\frac{dp}{dx}\right)y^2+ay+b \qquad (3.8)$$

When a viscous fluid moves over a solid surface it cannot slip over the surface. The fluid in immediate contact with the surface is at relative rest with respect to the surface. This is called as the no slip condition. At y=0, u=0 by the no slip condition. Therefore, b=0. Again at y=h, u=0 for the same reason. Therefore,

$$a = -\frac{1}{2\mu}\left(\frac{dp}{dx}\right)h$$

Hence

$$u = \frac{1}{2\mu}\left(\frac{dp}{dx}\right)y^2 - \frac{1}{2\mu}\left(\frac{dp}{dx}\right)hy = \frac{1}{2\mu}\left(\frac{dp}{dx}\right)\left(y^2 - hy\right) \tag{3.9}$$

From the above equation it is evident that the velocity varies parabolically across the flow. Also, the velocity varies directly as the pressure gradient. As the gradient increases, so does the velocity. Location of the maximum velocity can be found by

$$\frac{\partial u}{\partial y} = \frac{1}{2\mu}\left(\frac{dp}{dx}\right)\left(2y - h\right) = 0$$

Hence the maximum velocity occurs at y=h/2, i.e., at the mid plane. The velocity profile is parabolic and is therefore symmetric about the centerline of the flow. The maximum velocity can be evaluated by substituting y=h/2 in Equation (3.9). It is found to be

$$u_{max} = -\frac{h^2}{8\mu}\left(\frac{dp}{dx}\right) \tag{3.10}$$

In the above equation u_{max} is a positive quantity. Hence $\left(\frac{dp}{dx}\right)$ is a negative quantity. This means that a positive maximum velocity exists if the pressure is decreasing in the direction of the flow. Velocity gradient at the wall has to be obtained in order to evaluate the wall shear stress. Using Equation (3.9) obtain the velocity derivative and substitute y=0 or h to find the wall shear stress.

$$\tau_{wall} = \mu\left(\frac{\partial u}{\partial y}\right)_{wall} = -\frac{h}{2}\left(\frac{dp}{dx}\right) = \left(-\frac{h}{2}\right)\left(-\frac{8\mu u_{max}}{h^2}\right) = \frac{4\mu u_{max}}{h} \tag{3.11}$$

Average flow velocity can be defined in terms of the maximum velocity as follows

$$u_{av} = \frac{1}{h}\int_0^h u dy = \frac{1}{2\mu h}\left(\frac{dp}{dx}\right)\int_0^h \left(y^2 - hy\right) dy = -\left(\frac{1}{2\mu h}\right)\left(\frac{8\mu u_{max}}{h^2}\right)\left(-\frac{h^3}{6}\right) = \frac{2}{3}u_{max} \tag{3.12}$$

Local skin friction coefficient is defined as

$$C_f = \frac{\tau_{wall}}{\frac{1}{2}\rho u_{av}^2} = \frac{\frac{4\mu u_{max}}{h}}{\frac{1}{2}\rho u_{av}^2} = \frac{12\mu}{\rho u_{av} h} = \frac{12}{Re}, \text{ where } Re = \frac{\rho u_{av} h}{\mu} \tag{3.13}$$

The above expression is found to be valid for lower Reynolds numbers. At higher Reynolds numbers transition to turbulent flow occurs and the above analysis is no longer valid.

It is worth noting that the velocity distribution for this flow problem was obtained from basic principles by considering equilibrium of forces acting on a fluid element. It could have been obtained from the governing flow equations directly as follows.

Let us consider the incompressible continuity equation in its differential form. Referring back to Equation (1.19), if we consider the flow to be steady, the first term $\frac{\partial \rho}{\partial t}$ becomes zero. If we further consider the flow to be incompressible then the equation becomes $\nabla.\left(\rho\vec{V}\right) = \rho\nabla.\vec{V} = 0$. In two dimensional Cartesian coordinates this equation can be written as

$$\frac{\partial u}{\partial x} + \frac{\partial v}{\partial y} = 0 \tag{3.14}$$

Since the flow is parallel in the case of two dimensional Poiseuille flow, v=0, hence, $\frac{\partial v}{\partial y} = 0$. From the above equation,

$$\frac{\partial u}{\partial x} = 0 \tag{3.15}$$

hence u does not vary with x, it varies only along y. The differential form of x-momentum equation is given by Equation (1.32). We write it down in the context of incompressible flow as follows, where $\left(\overrightarrow{F_x}\right)_{viscous}$ has been replaced by its exact form.

$$\frac{\partial u}{\partial t}+\nabla.\left(u\vec{V}\right)=-\frac{1}{\rho}\frac{\partial p}{\partial x}+\overrightarrow{B_x}+\nu\nabla^2 u$$

If we assume the flow to be steady and devoid of body forces the x-momentum equation reduces to

$$\nabla.\left(u\vec{V}\right)=-\frac{1}{\rho}\frac{\partial p}{\partial x}+\nu\nabla^2 u \tag{3.16}$$

By applying equation (3.14) the left hand side term of the above equation can be simplified as

$$\frac{\partial\left(u^2\right)}{\partial x}+\frac{\partial\left(uv\right)}{\partial y}=2u\frac{\partial u}{\partial x}+u\frac{\partial v}{\partial y}+v\frac{\partial u}{\partial y}=u\left(\frac{\partial u}{\partial x}+\frac{\partial v}{\partial y}\right)+u\frac{\partial u}{\partial x}+v\frac{\partial u}{\partial y}=u\frac{\partial u}{\partial x}+v\frac{\partial u}{\partial y}$$

Therefore Equation (3.16) can be written in two different forms as follows

$$\frac{\partial(u^2)}{\partial x}+\frac{\partial(uv)}{\partial y}=-\frac{1}{\rho}\frac{\partial p}{\partial x}+\nu\nabla^2 u \tag{3.17a}$$

$$u\frac{\partial u}{\partial x}+v\frac{\partial u}{\partial y}=-\frac{1}{\rho}\frac{\partial p}{\partial x}+\nu\nabla^2 u \tag{3.17b}$$

Equation (3.17a) is the conservative form and (3.17b) the non-conservative form. We would be using the non-conservative form for the present case. We also need the y-momentum equation, so we write it down as follows

$$u\frac{\partial v}{\partial x}+v\frac{\partial v}{\partial y}=-\frac{1}{\rho}\frac{\partial p}{\partial y}+\nu\nabla^2 v \tag{3.18}$$

Since v and its derivatives are zero throughout the flow field for this problem, from the above equation $\frac{\partial p}{\partial y}=0$. Hence pressure is purely a function of x and hence the pressure gradient in the x-momentum equation is written as $\frac{dp}{dx}$. Substituting Equation (3.15) in Equation (3.17b) we get

$$0=-\frac{1}{\rho}\frac{dp}{dx}+\nu\frac{d^2u}{dy^2}$$

On integrating the above equation and applying the no slip boundary conditions we would get back Equation (3.9) again. Therefore both the approaches give identical result as expected.

3.2.2 Couette Flow

Couette flow is a flow between two parallel flat plates, one of which is at rest and the other moving with a velocity U parallel to the fixed plate. A two dimensional incompressible constant temperature viscous flow would be established between the two plates driven by the moving plate. Note that this flow would not be possible if the fluid was inviscid! That is because the moving plate in an inviscid fluid would not be able to drag the flow through the action of shear stress because the viscosity coefficient of such a fluid is zero.

We start by applying the Equation (3.8) to obtain the velocity distribution between the two parallel plates by implementing suitable boundary conditions on the respective plate surfaces. This is perfectly valid because the same forces as shown in Figure 3.2 would exist in general on a fluid element for this problem. We assume initially that both pressure and viscous forces exist in the flow.

$$u = \frac{1}{2\mu}\left(\frac{dp}{dx}\right)y^2 + ay + b \tag{3.8}$$

The no-slip boundary conditions may be written as

u = 0 at y = 0, which gives b = 0

u = U at y = h, which gives

$$U = \frac{h^2}{2\mu}\left(\frac{dp}{dx}\right) + ah$$

or, $a = \frac{U}{h} - \frac{h}{2\mu}\left(\frac{dp}{dx}\right)$

Substituting the values of a and b in the velocity distribution expression gives

$$u = \frac{y^2}{2\mu}\left(\frac{dp}{dx}\right) + \frac{Uy}{h} - \frac{hy}{2\mu}\left(\frac{dp}{dx}\right)$$

$$= \frac{Uy}{h} + \frac{1}{2\mu}\left(\frac{dp}{dx}\right)\left(y^2 - hy\right)$$

$$\frac{u}{U} = \frac{y}{h} + \alpha \cdot \frac{y}{h}\left(1 - \frac{y}{h}\right) \tag{3.19}$$

α is the non-dimensional pressure gradient given by

$$\alpha = -\frac{h^2}{2\mu U}\left(\frac{dp}{dx}\right) \tag{3.20}$$

For $\alpha > 0$ the pressure decreases in the direction of flow. Hence the velocity is positive over the whole width between plates.

For $\alpha < 0$ pressure increases in the direction of flow. Reverse flow begins to occur near the stationary wall where the adverse pressure force is stronger than viscous force.

For $\alpha = 0$ fluid motion is purely due to viscous force. This flow is called simple Couette flow.

In this case $u = \frac{y}{h}U$, which implies that the velocity variation is linear within the gap.

Maximum velocity occurs at the position of y where slope of velocity is equal to zero.

$$\frac{\partial u}{\partial y} = 0 = \frac{U}{h} + \frac{\alpha U}{h}\left(1 - \frac{2y}{h}\right)$$

The position of maximum velocity is given by

$$\frac{y}{h} = \frac{1}{2} + \frac{1}{2\alpha}$$

The reader is encouraged to obtain an expression for maximum velocity.

The average velocity is found by the same procedure applied in the previous section as follows

$$u_{av} = \left(\frac{1}{2} + \frac{\alpha}{6}\right)U \tag{3.21}$$

For $\alpha = 0$, i.e., simple Couette flow, $u_{av} = U/2$,

$$\text{Volumetric flow } Q = h.\, u_{av} = \left(\frac{1}{2} + \frac{\alpha}{6}\right) Uh \tag{3.22}$$

Shear stress is obtained as

$$\tau_{yx} = \mu \frac{du}{dy} = \mu \frac{U}{h} + \frac{\mu U \alpha}{h}\left(1 - \frac{2y}{h}\right) \tag{3.23}$$

for simple Couette flow $\alpha=0$, $\tau_{yx} = \dfrac{\mu U}{h} = \text{constant}$.

Till date, no exact solution exists for the full Navier Stokes equations. However, under suitable simplifications, it is possible to obtain exact solutions of Navier Stokes equations. Apart from the two flow problems discussed here, there are several other viscous flow problems for which exact solutions are available. For such details the reader is encouraged to refer the books of Schlichting (1979), White (1991), Drazin & Riley (2007) etc.

3.3 Introduction to Boundary Layer

3.3.1 The basic concept

When a viscous fluid moves over a solid surface the relative velocity increases from zero at the surface to the velocity in the free stream through a layer of fluid which is called the boundary layer. The concept of boundary layer is a mathematical one, which divides the flow region into two parts - one outside the boundary layer and the other inside the boundary layer. The rate of change of velocity with distance from the surface $\left(\frac{\partial u}{\partial y}\right)$ is large inside the boundary layer and small outside it. The viscous stress which is related to the velocity gradient is therefore large only inside the boundary layer, elsewhere it is small. Consequently, flow inside the boundary layer is highly viscous whereas the flow outside it can be treated as inviscid. The governing equation of flow outside the boundary layer is therefore Laplace equation while that for inside the boundary layer is the Navier-Stokes equation. When we consider flow past a flat plate or an airfoil, over the forward part of the surface, the flow in the boundary layer is laminar, that is, it is smooth and proceeds roughly parallel to the surface in streamlines. At one stage transition takes place to turbulent flow. In turbulent motion there is a general mean motion roughly parallel to surface but in addition there are rapid random fluctuations in velocity in both direction and magnitude. In laminar flow the skin friction drag is lower than in turbulent flow. Turbulent flow does not separate from the surface easily because it can draw energy from the mainstream flow through vigorous mixing which is one of its intrinsic characteristic. On the contrary, laminar flow separates easily under the influence of adverse pressure gradient. Factors which are favorable for maintenance of laminar flow are low turbulence free stream flow, favorable pressure gradient $\left(\frac{dp}{dx}\right) < 0$, low Reynolds number, smooth surface etc. Adverse pressure gradient $\left(\frac{dp}{dx}\right) > 0$ induces separation. In general, for incompressible flows, as flow area reduces, flow accelerates and consequently leads to favorable pressure gradient and vice versa. Consider incompressible flow past a two dimensional circular cylinder. In the front half of the cylinder flow accelerates and therefore favorable pressure gradient exists, whereas in the rear half flow decelerates and consequently the pressure gradient is adverse. Thus the flow is more susceptible to separation in the rear half. Increase in adverse pressure gradient leads to decrease in velocity gradient near the wall. This was observed in the case of Couette flow. In adverse pressure gradient situations a stage may be reached when $\left(\frac{\partial u}{\partial y}\right)_{wall}$ reduces to zero. The flow is then on the verge of separation. This means it is no longer able to follow the body surface as it has to encounter higher pressure than it can sustain. Therefore it takes a path along which it can sustain its motion and thereby leaves the body surface and approaches the free stream. The boundary layer ceases to exist beyond this point. At the separation point the wall shear stress becomes zero. The body surface downstream of this point is called as separated flow region and the region of fluid which surrounds it is called wake. Downstream of the separation point the velocity gradient becomes negative and so does the shear stress. The momentum dissipated due to flow separation is quite large and it gives rise to a high drag. Using a Pitot tube rake if the velocity distribution in the wake region of the body is obtained a deficit in momentum is found in the wake flow compared to the upstream uniform flow. This deficit in momentum is equal to the drag force acting on the body.

In boundary layer calculations interest is rarely in the accurate calculation of velocity profiles or the thickness of boundary layer. This is because it is quite impractical to ascertain the thickness over which the velocity recovers back to free stream value exactly, because that is an impractically large distance. It is observed from experiments that the velocity growth rate is highest near the wall and it decreases rapidly with increase in wall distance. The velocity asymptotically approaches free stream value over a significantly large distance. Therefore, for all practical purposes, the boundary layer thickness δ is defined as that thickness over which 99% of free stream value is recovered. Therefore, in boundary layer calculations, interest is often limited to calculating certain representative boundary layer parameters e.g., displacement thickness δ^*, momentum thickness θ, energy thickness δ_E, local and overall skin friction coefficients C_f and C_F respectively, etc.

The laminar boundary layer equations are a set of simplified equations which were derived from Navier Stokes equations through an order of magnitude analysis performed by Prandtl. These equations are thus popularly known as Prandtl's boundary layer equations. These can be further simplified for certain problem cases. For example, their simplified form for solving boundary layer flow past a flat plate is given by Blasius equation which is a third order non linear ordinary differential equation.

3.3.2 Boundary Layer Parameters

(a) Displacement thickness

This is defined as the thickness by which fluid outside the boundary layer is displaced away from the boundary due to the existence of the layer. If there were no boundary layer the free stream velocity U_∞ would persist right down to the body surface. The reduction in volume flow rate due to reduction of velocity in the boundary layer is therefore

$$\delta Q=\int_0^h (U_\infty - u)dy \tag{3.24}$$

the dimension h being chosen so that $u = U_\infty$ for any value of y greater than h. If the volume flow rate is now considered to be restored by displacement of the streamline away from the surface to a position at a distance δ^* from the surface we have

$$\delta Q = U_\infty \delta^* \tag{3.25}$$

In other words, flow over a solid surface having a boundary layer of thickness δ, is equivalent to flow with no boundary layer over a solid surface of thickness δ*

Equating the results of Equations (3.24) and (3.25) gives

$$\delta^* = \frac{1}{U_\infty}\int_0^h (U_\infty - u)dy = \int_0^h (1 - \frac{u}{U_\infty})dy \tag{3.26}$$

Now h is any arbitrary value which satisfies the following condition

$u = U_\infty$

or, $1 - u / U_\infty = 0$

for all values of y greater than h. The value of h may therefore be increased indefinitely without affecting the value of integral. So h may be allowed to increase towards infinity, viz h $\rightarrow \infty$ and the result obtained is

$$\delta^* = \int_0^\infty (1 - u/U_\infty)dy \tag{3.27}$$

In the practical measurement of δ* from a measured velocity distribution the infinite upper limit presents no difficulty. Measurements are made up to locations where non zero values of the term under the integral exist, thereby contributing to the value of δ^* .

(b) Momentum Thickness

Momentum thickness is given by

$$\theta = \int_0^\infty \frac{u}{U_\infty}(1 - \frac{u}{U_\infty})dy \tag{3.28}$$

Here, $\rho U_\infty^2 \theta$ represents the defect in the rate of transport of momentum in the boundary layer as compared with the rate of transport of momentum in the absence of boundary layer.

(c) Energy Thickness

$$\delta_E = \int_0^\infty \frac{u}{U_\infty}\left[1 - \left(\frac{u}{U_\infty}\right)^2\right]dy \tag{3.29}$$

Here, quantity $\rho U_\infty^3 \cdot \delta_E / 2$ represents the defect in the rate of transport of kinetic energy in the boundary layer when compared with the rate of transport of kinetic energy in the absence of the boundary layer.

Example 3.1

The velocity profile for a laminar boundary layer developing on a flat plate is given by

$u = a\sin(by) + c$

Apply suitable boundary conditions and therefore evaluate the constants a,b and c

The boundary conditions for this problem are:

(a) At y=0, u=0 (no slip condition)
(b) At y=δ, u=U_∞ (free stream condition)
(c) At y=δ, $\frac{\partial u}{\partial y} = 0$ (zero shear condition)

Applying (a) we get c=0

Applying (b) we get $u(\delta) = a\sin(b\delta) = U_\infty$

Applying (c) we get $\left.\frac{\partial u}{\partial y}\right|_{y=\delta} = ab\cos(b\delta) = 0$

Therefore $b\delta = \frac{\pi}{2}$, or $b = \frac{\pi}{2\delta}$

Substituting the above value of b in the equation for $u(\delta)$ we get

$$u(\delta) = a\sin(b\delta) = a\sin\left(\frac{\pi}{2}\right) = a = U_\infty$$

Hence, to sum up, the values of the constants are as follows:

$a = U_\infty$, $b = \frac{\pi}{2\delta}$, c=0 and the boundary layer velocity profile can be written as $u = U_\infty \sin\left(\frac{\pi y}{2\delta}\right)$

3.4 Multiple Choice Questions

1. In a Newtonian fluid flow shear stress is proportional to
a) density gradient
b) strain
c) pressure gradient
d) strain rate

2. At flow separation point on the body surface
a) $u > 0, v < 0, \frac{\partial^2 u}{\partial y^2} < 0$
b) $u = 0, v = 0, \frac{\partial u}{\partial y} = 0$
c) $u = 0, v = 0, \frac{\partial^2 u}{\partial y^2} = 0$
d) $u = 0, v = 0, \frac{\partial u}{\partial y} < 0$

3. Two layers of fluids of different density and viscosity are flowing one over the other down a flat plane which is kept at an angle with the horizontal. At the interface of the two fluid layers
a) pressure would be equal to atmospheric pressure
b) shear stress would be equal
c) velocity would be equal
d) shear stress would be zero
4. If the Reynolds number in a boundary layer flow decreases
a) Mach number increases
b) Pressure gradient normal to the body surface decreases
c) Boundary layer thickness increases
d) Boundary layer thickness decreases

5. Under adverse pressure gradient a viscous flow can be assisted to remain attached to the boundary by
a) Moving the boundary tangential to the flow and along flow direction
b) Vibrating the boundary normal to the flow direction
c) Moving the boundary tangential to the flow and opposite to the flow direction
d) Injecting high momentum fluid into the flow tangentially

6. In the study of incompressible boundary layer the following parameters are important
a) Mach number and Reynolds number
b) Prandtl number and Reynolds number

c) Mach number
d) Reynolds number

7. The pressure gradient along the flow direction for viscous flow past a flat plate
a) increases
b) decreases
c) remains constant
d) is zero

8. The pressure gradient normal to the body surface for a boundary layer flow is
a) <0
b) >0
c) 0
d) constant

3.5 Figures

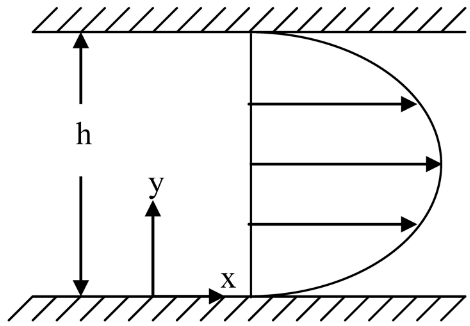

Figure 3.1 Velocity profile for two dimensional Poiseuille flow

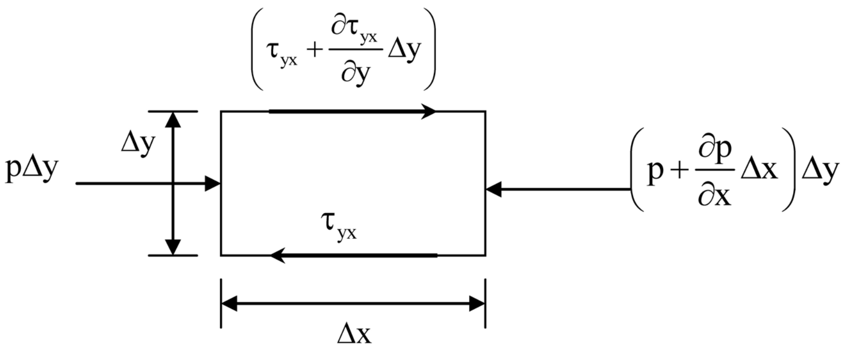

Figure 3.2 Forces acting on the two dimensional fluid element

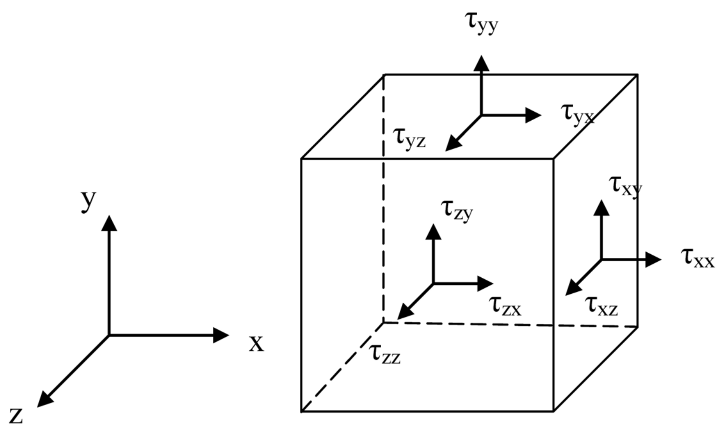

Figure 3.3 Shear and normal stresses caused by viscous action on a fluid element

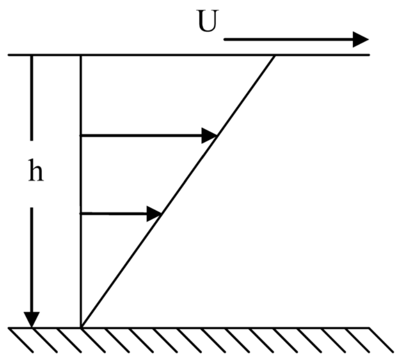

Figure 3.4 Velocity profile for two dimensional Couette flow

4 Wind Tunnels and a Few Basic Experiments

4.1 Introduction

Wind tunnels are instruments in which air flow is generated in a test section over a design speed range and losses caused by air flow through the tunnel are minimized in order to ensure efficient operation of the tunnel. The test section should be able to accommodate various kinds of models which need to be tested to determine their aerodynamic characteristics. It may involve flow visualisation using various means like smoke, tuft, laser sheet etc, pressure measurement using manometer, pressure sensor, pressure sensitive paint etc, measurement of forces and moments using mechanical balance or strain gauges. The balance may be kept outside the test section or inside it. Accordingly, it is called as external or internal balance. The prerequisites for the usability of wind tunnels for aerodynamic investigations are the following:

1. The similarity laws can be applied, so that the results obtained with models in the wind tunnel can be transferred to flows about full-scale configurations, especially to flows about aircrafts in free flight. In general, complete similarity is very difficult to attain in a single experiment. For this reason, it is necessary to determine the similarity parameter which is of greatest importance for the problem to be investigated, and only obey the corresponding similarity law in the experiment. In aerospace applications the two most important similarity parameters are Mach number and Reynolds number.

2. The boundary conditions for the flows about the models in the wind tunnel and the full-scale configurations have to be similar. If necessary, the experimental results have to be corrected by applying suitable boundary corrections.

Instrumentation plays a vital role in wind tunnel testing. The accuracy of experimental results depends not only on the quality of the tunnel but also on the performance of the measuring equipments. It is often important to measure the pressure distribution on model surface and also the overall forces and moments acting on the model. Velocity is general can be calculated from pressure and need not be measured directly. However, it may be required to directly measure fluctuations in the velocity field in turbulent flow. Sometimes it may be also be necessary to make direct measurement of skin friction coefficient. To measure the above quantities suitable instrumentation is necessary. They could be broadly classified as two types, namely, mechanical and electronic. Examples of mechanical type instruments are liquid level manometers for pressure measurement and wind tunnel mechanical balances for measurement of overall forces and moments. However, such instrumentation lack fast response, and high data acquisition rate required for unsteady and transient measurements. Electronic instrumentation is therefore necessary to meet such requirements. A typical electronic measurement system may comprise of transducer or sensor, signal conditioner and a data acquisition system. The transducer senses the physical quantity under measurement which may be pressure or force and delivers a proportionate electrical signal to the signal conditioner. The signal is amplified, filtered and made acceptable for the data acquisition system by the signal conditioner. The data acquisition system could be an oscilloscope, digital display unit, PC etc. Though electronic systems are in wide spread use in modern wind tunnels it is first necessary to understand the basic principles which are often learnt more easily using mechanical instrumentation.

4.2 Low Speed Wind Tunnels

Wind tunnels for low speeds with air as working medium at atmospheric temperature and test section velocity less than around 100 m/s are usually continuously operated. Usually an axial fan generates a flow through the tunnel for fairly long duration so that extensive tests can be carried out on models. Two basic types of low speed wind tunnels are commonly in use:

4.2.1 Open Circuit Wind Tunnel

In this type of low speed wind tunnel air is drawn from the surrounding into the tunnel inlet, passed through the test section at relatively high speed and low pressure and then exhausted into the surrounding air through the tunnel outlet. The fan is usually placed near the outlet of the tunnel. Since the wind tunnel circuit is open, the working medium is not recirculated. The test section of the tunnel is generally closed, i.e., it is not open to atmosphere. However, if necessary, it could also be of open type. Air is drawn from the surrounding through a bell mouthed inlet which leads to a settling chamber with large cross sectional area and equipped with honeycomb shape flow straighteners and screens. It is important to generate a uniform velocity profile with low turbulent intensity in the test section. This is achieved with the help of flow straighteners and screens located in the settling chamber. Relatively low velocity in the settling chamber leads to small losses. This is because losses scale directly with local dynamic pressure. The settling chamber is followed by a contraction section and then followed by a test section. A high contraction ratio between settling chamber and test section yields a large velocity in the test section which is desirable for model testing purposes. For closed test sections the pressure is below atmospheric and the flow speed is maximum. A diffuser is used downstream of the test section for effective pressure recovery. Most often the fan is mounted towards the end of the diffuser, which is also the end of the wind tunnel. From the inlet to the test section the cross section is usually square or rectangular. Starting portion of the diffuser has a square/rectangular-to-circular transition section required to house the circular fan downstream. A long diffuser enables a high pressure recovery, but this is also associated with higher construction costs and higher wall friction losses. In a long diffuser the divergence angle can be kept low and therefore the adverse pressure gradient is lower. This is more favorable for an efficient pressure recovery without flow separation. Large pressure recovery in the diffuser leads to reduced power requirement for driving the fan and consequently lower operating cost. The advantages of this type of tunnel are its simple and low cost construction and easier maintenance.

4.2.2 Closed Circuit Wind Tunnel

In these low speed wind tunnels air is circulated in a closed loop within the wind tunnel circuit. Figure 4.1 shows a typical closed circuit low speed wind tunnel. We would look at various sections of the circuit and discuss briefly about their functions here. When the fan is operated, air flows in counter clockwise direction through the wind tunnel circuit. Section 1 is the test section where models are located for various aerodynamic measurements. The dimensions of the test section should be adequate to house the models and locate the instruments for measurement. The test section should have adequate lighting, windows for easy access and preferably transparent walls for good visibility. This section of the tunnel has the minimum cross-sectional area and therefore, the highest velocity. The average dynamic pressure in this section is used to scale the energy losses for the test section and the net energy losses for the complete wind tunnel circuit. Section 2 is the first diffuser section. The function of the diffuser is to decelerate the flow with minimum energy loss and the maximum static pressure recovery. Deceleration of the flow downstream of the test section is useful in minimizing the energy losses which are proportional to the average dynamic pressure in the other sections. Section 3 contains the first and second corners for the closed-circuit wind tunnel. It also acts as the second diffuser section. The corners of this section include the turning vanes which help to minimize the turbulence and losses produced by the 180 degree change of flow direction and also produce a more uniform velocity distribution. Section 4 is a rectangular-to-circular transition section required to mate to the circular fan housed in Section 5. Unlike all other sections of the wind tunnel, the fan provides a net energy gain. In fact the rate of energy addition at the fan is exactly equal to the combined rate of energy loss in all other sections. Section 6 is the third diffuser which provides additional deceleration of the flow. This section also provides a transition from a circular to a rectangular cross section. Section 7 contains the third and fourth corners of the wind tunnel circuit. As in section 3, these corners contain turning vanes to facilitate an efficient change of direction for the flow. This section also acts as the fourth diffuser. Section 8 is referred to as the settling section. It contains honeycomb material to straighten or break up the largest turbulent eddies in the flow. Different honeycomb geometries may be chosen to achieve the desired flow properties before the flow reaches the test section. The honeycomb is followed by one or more fine mesh screens. The screens have two primary functions. First, they produce a flow resistance proportional to the local dynamic pressure which results in a more uniform velocity distribution across the cross section. Second, the medium scaled turbulent eddies generated by the honeycomb are further broken into smaller turbulent eddies with scales of the order of the screen mesh size. These small scale eddies have a high viscous dissipation rate and decay rapidly downstream of the screens. The flow resistance of the honeycomb and screens are greater than any other section of the tunnel. The corresponding rate of energy loss, however, is minimized by decelerating the flow through the diffusers so that the average velocity in the settling section is a small fraction of the velocity in the test section depending on the area ratio between these two sections. Section 9 is the contraction section. The flow is accelerated back to the test section velocity as the cross sectional area is reduced. Usually higher order polynomial curves are used to design the contraction section geometry.

As mentioned before, when the flow moves through the wind tunnel circuit losses are incurred. This is reflected through the loss of total pressure in each section. If total pressure losses for all the sections are summed up, we get the net total pressure loss in the circuit given by the following equation

$$(\Delta p_0)_{loss} = \sum_{j=1,N}\left[\left(p_i + \frac{1}{2}\rho V_i^2\right) - \left(p_e + \frac{1}{2}\rho V_e^2\right)\right]_j = \sum_{j=1,N} k_j \left(\frac{1}{2}\rho V_{i,j}^2\right) \tag{4.1}$$

The subscript 'i' stands for inflow station of a section and 'e' stands for exit station of the section respectively. 'k_j' stands for loss coefficient for the j^{th} section. By using Continuity equation the velocity at each location of the tunnel can be correlated with that in the test section by using the area ratio between these two stations as follows

$$A_{i,j} V_{i,j} = A_t V_t \tag{4.2}$$

or, $V_{i,j} = \dfrac{A_t}{A_{i,j}} V_t$

where subscript 't' stands for test section. By substituting Equation (4.2) in Equation (4.1) we get

$$(\Delta p_0)_{loss} = \left(\frac{1}{2}\rho V_t^2\right)\sum_{j=1,N} k_j\left(\frac{A_t}{A_{i,j}}\right)^2$$
$$= \frac{1}{2}\rho V_t^2 K$$

$$\text{where } K = \sum_{j=1,N} k_j\left(\frac{A_t}{A_{i,j}}\right)^2 \tag{4.3}$$

By the above approach loss coefficient for each wind tunnel section is used to determine a single effective loss coefficient K for the complete tunnel. The increase in total pressure across the fan must be equal to net total pressure loss across other sections of the tunnel. Since the fan section has a constant cross-sectional area, the jump in total pressure across the fan is equal to the static pressure jump across it. The power loss in the wind tunnel circuit is given as a product of static pressure loss (Δp_{loss}) and flow rate (Q)

$$P_{loss} = \Delta p_{loss} Q = \left(\frac{1}{2}\rho V_t^2 K\right)(A_t V_t) = \frac{1}{2}\rho A_t V_t^3 K \tag{4.4}$$

Wind tunnel performance is quantified using a ratio of energy flux in the test section to the rate of energy supply or power input to the fan. This ratio is called as the energy ratio (ER) of the Wind Tunnel. This can typically range from 3 to 7 for most closed test section low speed wind tunnels.

$$ER = \frac{\frac{1}{2}\rho A_t V_t^3}{\frac{1}{2}\rho A_t V_t^3 K} = \frac{1}{K} \tag{4.5}$$

4.3 Supersonic Wind Tunnels

The nozzle of a supersonic wind tunnel is usually designed with Method of Characteristics (MOC), details of which are well elaborated in Shapiro (1953), Zucrow and Hoffmann (1976), etc. The purpose of the nozzle is to accelerate the flow gradually from very low speed as it comes into the nozzle from the settling chamber to sonic speed in the throat of the nozzle and further to a prescribed supersonic speed in the test section. The nozzle consists of the subsonic part, the transonic part, the expansion part, and the part for correction of the flow to uniform supersonic conditions in the test section. In the flow expansion zone there are several reflections along the wall of the nozzle. The expansion waves hitting the wall of the nozzle in the correction part are cancelled by equally strong compression waves generated due to concave contour of the wall. If the nozzle geometry is correctly designed, the flow in the test section is parallel and its

Mach number is constant. A change of the Mach number can only be achieved by changing the entire nozzle geometry. This can be realized with exchangeable nozzles or nozzles with variable contours. Nozzles used in supersonic tunnels are often referred to as De Laval nozzles.

After supersonic flow is established in the nozzle and measurements are performed on the models in the test section the flow is decelerated and pressure is recovered. This is achieved using a convergent-divergent diffuser. The pressure recovery should be as large as possible in order to keep the required compressor power as small as possible for continuously operating tunnels or to achieve optimum tunnel run time for intermittently operating tunnels. The largest pressure recovery is obtained, if critical flow conditions prevail in the throat of the diffuser and if the deceleration of the flow to subsonic conditions is facilitated by a weak normal shock in the divergent part of the diffuser, immediately downstream of the throat of the diffuser. Since the shock is weak, the losses caused by the shock are small. When the supersonic tunnel starts, a different cross section of the throat of the diffuser is required, as discussed below. During the initial phase of the start of the tunnel subsonic flow prevails in the entire tunnel. The speed of sound is first attained in the throat of the nozzle. The flow expands to supersonic speeds in the divergent part of the nozzle, with a normal shock terminating the supersonic part. With increasing velocity the shock moves downstream. The shock intensity and the losses in the flow reach their maximum when the shock is located in the test section. In order to guarantee that the mass flow can pass the diffuser, the cross section of the throat of the diffuser must then be sufficiently large. Several tunnels were built with an adjustable cross section of the throat of the diffuser, the size of which was reduced immediately after the start of the tunnel in order to guarantee a maximum pressure recovery.

There are several types of supersonic wind tunnels, namely, continuous tunnels, intermittent blow down tunnels and intermittent indraft tunnels. Continuous wind tunnels are essentially a closed-circuit system and can be used to achieve a wide range of Mach numbers. They are designed so that the air that passes through the tunnel does not exhaust to the atmosphere; instead, it enters through a return passage and is cycled through the test section repeatedly. This type of wind tunnel is beneficial because the operator has more control of the conditions in the test section, superior flow quality, quieter flow, longer run time etc. The disadvantages are long time (typically two hours or more) to reach desired pressure, complicated and expensive construction, model changes require depressurization of the tunnel or isolation of the test section from the remaining portions of the tunnel. Intermittent blow down tunnels are most commonly used. These tunnels use the difference in pressure between a pressurized tank and atmosphere to attain supersonic speeds in the test section. These tunnels are designed to discharge the flow to the atmosphere, so the pressure in the tank is greater than that of the environment. A compressor is used to fill up a tank to a desired pressure before the tunnel run. At the beginning of a run, valves are opened and the pressure differential causes air to flow in the direction of the lower pressure until the pressure difference is zero. The test section is positioned at the end of the supersonic nozzle. Many blow down tunnels have two throats, with the second throat being used to slow supersonic flow down to subsonic speeds before it discharges directly into the atmosphere. Advantages of these tunnels are they are easy to start, they are easy and cheap to construct, smaller loads act on models due to shorter start time. Disadvantages of these tunnels are shorter test time, noisy operation, measurement equipments should have shorter response times and therefore are costlier. Intermittent indraft wind tunnels use the pressure difference between a low pressure tank and the atmosphere to create a flow. A vacuum tank is pumped down to a very low pressure, and the other end of the tunnel is open to the atmosphere. When the desired vacuum pressure is reached, a valve is opened, and air rushes from outside the tunnel, through the test section, into the vacuum chamber. The end of the run occurs when the pressure differential is no longer great enough to drive the tunnel at the desired test section Mach number. The advantages of these tunnels are higher safety, almost constant stagnation temperature during operation, contaminant free flow, etc. Disadvantages are that they are several times more expensive and lower range of Reynolds number is achievable for same range of Mach number as compared to blow down tunnels.

4.4 Some Basic Experiments in Low Speed Wind Tunnels

In this section we are going to spend some time in learning how to design and perform a few basic experiments in a low speed wind tunnel. In the next section we will learn about a few basic experiments which could be performed in a supersonic tunnel.

Experiments in a low speed wind tunnel start with its initial calibration. This involves obtaining the relationship between the speed or rpm of the fan and the test section air velocity. Application of the Pitot static tube was explained in Chapter 1 (Equation 1.38 and Figure 1.14) in obtaining air flow velocity. This instrument would be placed at the middle of the wind tunnel test section and its stagnation and static ports would be connected to two limbs of a manometer. The stagnation pressure being the highest pressure in the flow field would exceed the static pressure when the tunnel is running. Thus the liquid level in the limb connected to the stagnation port would go lower than the liquid level in the static pressure limb. If the difference in height between the liquid columns is Δh, density of the liquid is ρ_1, then we can write

$$p_0 - p_\infty = \Delta h \rho_1 g \tag{4.6}$$

Therefore equation (1.38) can be written as

$$U_\infty = \sqrt{\frac{2\Delta h \rho_1 g}{\rho_\infty}} \tag{4.7}$$

By running the wind tunnel at different discrete speed settings the above explained calibration could be performed.

A velocity boundary layer forms along the walls of the wind tunnel due to the viscous nature of the flow. The boundary layer at higher Reynolds number is a turbulent one. It is interesting to find out the variation of velocity within the boundary layer and therefore obtain various boundary layer parameters like displacement thickness, momentum thickness, etc which were discussed in Chapter 3. Usually the wind tunnel boundary layer thickness could vary from a few millimeters to a few centimeters depending on flow conditions and measurement location along the length of the tunnel. A very thin flat Pitot static tube mounted on a traverse mechanism with attached micrometer could be used for boundary layer measurements. Distance of the Pitot tube from the wall can be controlled precisely by the micrometer subject to its least count. Initially the bottom part of the flat tube should just touch the wall. In this position the probe is located nearest to the wall. If the tube thickness is 't', then the first measurement is recorded at a distance t/2 from the wall. If t=0.5 mm, the first measurement point would be 0.25 mm from the wall. The micrometer should be used to precisely control the movement of the probe away from the wall and measurements made at frequent intervals when the probe is close to the wall. This would ensure accurate measurement of the velocity profile within the boundary layer. The probe is made to traverse to such distances away from the wall where at least two to three consecutive measurements at increasing wall distance yields no perceivable change in the manometer readings. Essentially one would observe that stagnation pressure changes from a low value near the wall to its maximum value at the free stream but static pressure remains constant.

Another interesting experiment is to obtain the pressure distribution on a two dimensional geometry like an airfoil or a circular cylinder. To start with, the circular cylinder model would be easier to fabricate. For example standard circular metal pipes with good surface finish may be used for the purpose. The model should stretch from one end to the other of the test section and mounted suitably at the walls. It would be set across the flow direction. Small pressure ports would have to be made on the surface of the model. Thin pressure tubes housed inside the model would be connected to these ports on one end and to metallic adaptors kept outside the wind tunnel on the other. These metallic adaptors have a small diameter metal tube on one side which matches with the small diameter polythene tubes coming from the model end and a larger threaded end which can hold bigger diameter polythene tubes which are connected to the limbs of a multi tube manometer for pressure measurement. When the tunnel is operated the pressure variation on the cylinder surface would be recorded by the pressure ports. A port would have to be located at the front stagnation point of the cylinder which records the stagnation pressure (p_0) and another port on the wall of the tunnel which records the free stream static pressure (p_∞). Using these two pressures, the pressure at any other port on the model could be expressed in terms of a pressure coefficient as follows

We repeat Equation (1.3) here, now expressed in terms of the measured quantities directly

$$C_p = \frac{p - p_\infty}{q_\infty} = \frac{p - p_\infty}{p_0 - p_\infty} \tag{4.8}$$

It is interesting to compare the variation of pressure coefficient with θ, which is the angle measured from the front stagnation point of the cylinder. It is observed that the experimental pressure distribution matches fairly well with the theoretical pressure distribution given by

$$C_p = 1 - 4\sin^2\theta \tag{4.9}$$

near the stagnation region, i.e., when θ is close to 0° or 360°. Due to viscous action, there is large flow separation in the rear portion of the cylinder (as discussed in Chapter 3), thereby leading to a very different pressure distribution in that region as compared to the theoretical distribution. When the pressure distribution around the cylinder is integrated to find the resultant force, a net force is obtained along the flow direction called as drag force. The lift is zero for a symmetric geometry like circular cylinder but is non zero for a symmetric airfoil at non zero angle of attack or cambered airfoil at any angle of attack other than its zero lift angle of attack. The drag coefficient for a circular cylinder over a wide range of Reynolds number is of the order of 1.

4.5 Some Basic Experiments in Supersonic Wind Tunnel

Let us assume that we would use an intermittent blow down type supersonic wind tunnel for our experiment. In the first experiment a Pitot tube is inserted into the test section of a supersonic wind tunnel. The total pressure port is connected by a rubber tube to one limb of a multi tube mercury manometer. Wall static pressure is recorded from a point considerably upstream of the probe, which is similarly connected to another limb of the manometer. The working fluid in manometers used in low speed tunnels is usually water or water based fluids, whereas in supersonic tunnels it is a high density fluid like mercury. This is because the pressure variations in low speed flows are very small whereas they are very large in high speed flows. In order to keep the variation of liquid column levels within a reasonable range (so that the manometer height does not become excessively large) and at the same time have sufficient sensitivity of measurement, judicious choice of manometric fluid is necessary based on the tunnel speed. When supersonic free stream flow impinges on the probe, a detached bow shock is formed ahead of it because of its blunt nose. The shock is normal near tip of the probe. Therefore, pressure recorded by the Pitot tube is essentially the stagnation pressure behind a normal shock (say, $p_{0,2}$). If the measured wall static pressure upstream of the shock is p_1, then these two pressures are connected by a well known formula called as Rayleigh Pitot tube formula given as follows

$$\frac{p_{0,2}}{p_1} = \left(\frac{(\gamma+1)^2 M_1^2}{4\gamma M_1^2 - 2(\gamma-1)} \right)^{\frac{\gamma}{\gamma-1}} \left(\frac{1-\gamma+2\gamma M_1^2}{\gamma+1} \right) \tag{4.10}$$

Note that both the measured pressures should be expressed in absolute sense and not in a differential sense like was used in Equation (4.6). From the measured $p_{0,2}/p_1$ value using manometer obtain the value of M_1 from the above equation iteratively. This is nothing but the test section Mach number. When the tunnel is run, a constant $p_{0,1}$ is maintained at the reservoir using a suitable pressure regulating valve. A Bourdon pressure gage or some other suitable pressure gage mounted on the wall of the reservoir gives this pressure reading. From the pressure ratio $p_{0,1}/p_1$, assuming isentropic flow till before the Pitot tube induced shock we can compute M_1. Compare the two values of test section Mach number obtained by the above two different approaches. They should be clos e to each other.

Another interesting experiment can be planned with a wedge model of base height 'c' cm having a small semi wedge angle θ which is mounted in the test section of the supersonic wind tunnel at zero angle of attack. Typically 'c' should be such that the blockage effect on the flow is not more than a few percent. If the height of the test section of the tunnel is h cm then the blockage percentage is given by $(c/h)\times 100$. Note that the flow properties including the Mach number in the test section would depend on the blockage. From the earlier experiment one has a fairly good idea of the Mach number in the test section of the tunnel. Use the $\theta-\beta-M$ relation to check whether there would be an attached shock for this case. If not, then a wedge model of lower θ value has to be used such that an attached oblique shock is formed at its leading edge when the tunnel is operated. The wedge model should have adequate number of pressure measurement ports on its slanted surface as well as in its base region. Once the tunnel is run measure the pressure on the slanted surface and base region. Obtain the pressure coefficient using the following relation

$$C_p = \frac{2}{\gamma M_\infty^2}\left(\frac{p}{p_\infty} - 1\right) \tag{4.11}$$

Check whether your experimental results comply with the following observations:

a) The pressure on the slanted surface should be more or less constant. Compare this pressure coefficient with that predicted by oblique shock theory.
b) Due to flow expansion at the rear wedge corner, the pressure coefficient in the base region should be substantially lower than on the slant surface and should be more or less constant.

Use the measured pressure distribution around the wedge model to estimate its drag coefficient.

Another experiment may be planned with the same model to visualize the flow field characteristics using an optical device called as Schlieren system. This optical device is used to see density gradients in the flow. Since large density gradients occur at shock region they are seen as dark bands, while expansion fans are seen as weaker bright bands due to gradual change in density across them. The Schlieren system has a light source and a series of focusing lens, knife edge to cut off and control illumination and a projection plane on which image of the illuminated test section is focused. The observer can see this image. Light cannot pass through the model due to its opaqueness and therefore that portion of the image is dark. When the tunnel is not operating, the remaining portion of the image is uniformly illuminated. When the tunnel starts operating, the darker and lighter bands are formed in the image indicating formation of shock and expansion fan. Take a photograph of this image when the tunnel is in operation. From the photograph obtain the oblique shock wave angle and compare it with the value obtained from $\theta - \beta - M$ relation. Also look carefully at the flow features at the rear corner of the wedge and its base region and try explaining them.

4.6 Multiple Choice Questions

1. Air flows from a reservoir through a converging diverging nozzle at low subsonic speed and is exhausted into the atmosphere. A Pitot tube is mounted at the mid section of the nozzle and traversed along the length of the nozzle from exit to the reservoir end. The pressure recorded by Pitot tube will

a) increase during traverse
b) derease during traverse
c) will decrease up to the throat and then increase during traverse
d) will remain constant during traverse

2. A circular cylinder is mounted in the test section of a low speed wind tunnel. The pressure distribution around it is measured when the tunnel is running. Pressure distribution is integrated to obtain the drag coefficient, c_{d1}. The circular cylinder is then mounted on a device called external balance which holds it from outside the test section and can measure all the forces acting on it when the tunnel is running. From the reading of the balance the drag coefficient is obtained as c_{d2}. The two drag coefficient values obtained from the two separate measurements can be calculated as follows

a) $c_{d1} = c_{d2}$
b) $c_{d1} > c_{d2}$
c) $c_{d1} < c_{d2}$
d) $c_{d2} \approx 2c_{d1}$

3. For the same test section speed and flow rate efficiency of a closed circuit low speed wind tunnel is

a) Greater than that of an open circuit tunnel
b) Less than that of an open circuit tunnel
c) Equal to that of an open circuit tunnel
d) Not comparable with that of an open circuit tunnel because of the differences in design

4. A supersonic wind tunnel is operated first with a wedge mounted in its test section and then a cone mounted in its test section. Both of them have the same base height. Drag coefficient is obtained for both the bodies and found to be equal to c_{dw} and c_{dc} respectively. The two drag coefficients could be related as follows

a) $c_{d1} = c_{d2}$
b) $c_{d1} > c_{d2}$
c) $c_{d1} < c_{d2}$
d) $c_{d2} \approx 2c_{d1}$

5. The Schlieren technique works on the basis of
a) density variation in the flow field
b) pressure varitation in the flow field
c) velocity variation in the flow field
d) density gradient variation in the flow field

4.7 Figures

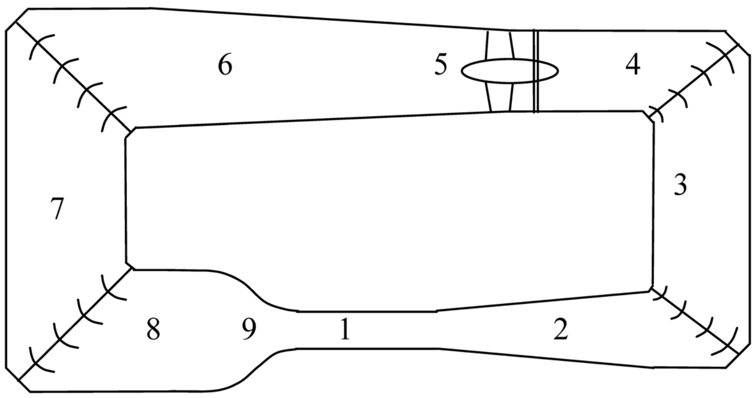

Figure 4.1 Layout of a low speed closed circuit wind tunnel

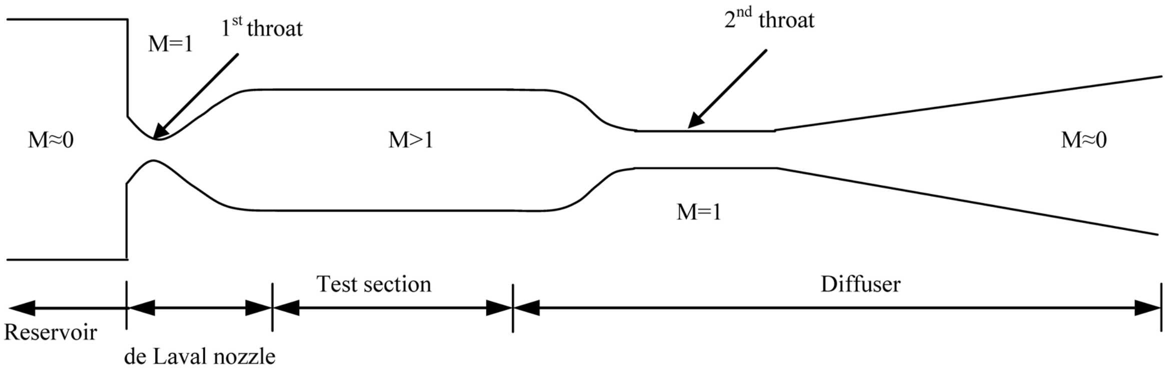

Figure 4.2 Layout of a blow down supersonic wind tunnel

References

J. D. Anderson, *Fundamentals of Aerodynamics,* 2d ed., Mc-Graw-Hill, New York, 1991.

J. D. Anderson, Jr., *Modern Compressible Flow, with Historical Perspective,* 2d ed., McGraw-Hill, New York, 1990.

J. D. Anderson, Jr., *Hypersonic and High Temperature Gas Dynamics,* McGraw-Hill, New York, 1989.

I. H. Abbott and A. E. von Doenhoff, *Theory of Wing Sections,*Dover, New York, 1959.

M. J. Zucrow and J. D. Hoffman, *Gas Dynamics Vol I and II*, John Wiley and Sons, 1976

A. H. Shapiro, *The Dynamics and Thermodynamics of Compressible Fluid Flow, Volumes 1 and 2*, The Ronald Press Company, New York, 1953

H. Schlichting, *Boundary Layer Theory,* 7th ed., McGraw-Hill, New York, 1979.

F. M. White, *Viscous Fluid Flow,* 2d ed., McGraw-Hill, New York, 1991.

P. Drazin and N. Riley, *The Navier-Stokes Equations, A Classification of Flows and Exact Solutions*, Cambridge University Press, 2007

J.B. Barlow, W.H. Rae, Jr and A. Pope, *Low Speed Wind Tunnel Testing*, John Wiley and Sons, 1999

A. Pope and K. L. Goin, *High Speed Wind Tunnel Testing*, John Wiley and Sons, 1965

R, J. Goldstein, Editor, *Fluid Mechanics Measurements*, Hemisphere, New York, 1983